REPORT No. 241

ELECTRICAL CHARACTERISTICS OF SPARK GENERATORS FOR AUTOMOTIVE IGNITION

By R. B. BRODE, D. W. RANDOLPH, and F. B. SILSBEE
Bureau of Standards

REPORT No. 241

ELECTRICAL CHARACTERISTICS OF SPARK GENERATORS [1] FOR AUTOMOTIVE IGNITION

By R. B. Brode, D. W. Randolph, and F. B. Silsbee

SUMMARY

This paper reports the results of an extensive program of measurements on 11 ignition systems differing widely in type. The results serve primarily to give representative data on the electric and magnetic constants of such systems, and on the secondary voltage produced by them under various conditions of speed, timing, shunting resistance, etc. They also serve to confirm certain of the theoretical formulas which have been proposed to connect the performance of such systems with their electrical constants, and to indicate the extent to which certain simplified model circuits duplicate the performance of the actual apparatus.

INTRODUCTION

For several years the Bureau of Standards has carried on a study of ignition systems for the National Advisory Committee for Aeronautics and other branches of the Federal Government. Much of this work has been devoted to the solution of special problems of immediate urgency, but throughout the work the need has been felt for the formulation of a systematic basic theory of operation of such apparatus, and whenever opportunity permitted the work has been directed toward the foundation of such a theory. National Advisory Committee for Aeronautics reports No. 58, "Characteristics of High Tension Magnetos," and No. 123, "Simplified Theory of the Magneto," together with Bureau of Standards Scientific Paper No. 424, "Mathematical Theory of Induced Voltage in the High Tension Magneto," constitute steps in this work. In 1922 a program of measurements was undertaken on a group of spark generators for the purpose of determining (1) their performance under various conditions of operation, (2) the electrical and magnetic characteristics of the apparatus, and (3) the extent to which the theoretical relations set forth in the reports listed above could be applied to these particular types of spark generators. The principal results of this investigation are here presented.

The ignition systems used in this work were all of the jump-spark type, and included both battery-coil and magneto systems. The systems were selected so as to give as great a variety as possible in the arrangement of the magnetic circuit. A detailed description of the systems will be found in the section under "Description of the spark generators studied," of this report. In considering the results of this work it should be borne in mind that the tests given cover only the electrical performance and not the mechanical quality of the apparatus, and furthermore that the data were all obtained with apparatus which was new and in good condition. In finally judging the relative merits of different types of spark generators such features as mechanical workmanship, resistance to wear, waterproofness, and other qualities which could be demonstrated only by protracted endurance tests are of great importance. These factors, however, have not been dealt with in the present paper. It should also be mentioned that, in order to cover apparatus differing as much as possible in the type of magnetic circuit, machines have been included which differ greatly in size and cost, and which would not normally enter into competition with one another in any single application. Still another point that should be

---

[1] Following British practice the term "spark generator" is here used to designate the electrical equipment which directly serves to produce the ignition spark; and includes both the high-tension magneto and the battery, induction coil, and breaker of a battery-coil system.

mentioned is that some of the magnetos give four sparks per revolution, while others give only two sparks per revolution. Magnetos of the former class are, in general, used with engines having a large number of cylinders, while the latter are used on engines of a smaller number of cylinders where the magneto is not necessarily required to operate at such high speeds relative to the engine crankshaft. This fact should be taken into account when making comparisons, as, for example, in the case of the curves showing crest voltage at slow operating speeds.

SPARK-GENERATOR REQUIREMENTS

The requirements for the satisfactory operation of a spark generator are as follows:

(a) It must produce sufficient voltage to break down the gap at the spark plug.

(b) Each spark must be capable of igniting an explosive mixture.

(c) The sparks must occur at the proper time in the engine cycle.

These requirements must be met under the following conditions:

1. At any speed within the normal range of engine operation.

2. While the system is shunted by the capacitance of the spark plug and connecting wires.

3. While the system is shunted by the conductance of the layer of carbon which may be deposited on the insulation of the spark plug.

Paterson and Campbell (Reference 1) have shown by experiments on gasoline-air mixtures that ignition will be produced provided the energy in the spark is not less than 0.00025 joule. The limiting energy depends considerably upon the sparking voltage of the gap, but it is found that if the capacitance has the smallest value which is likely to be met with in automotive equipment, and if the sparking voltage has the lowest value which is likely to occur with a spark plug of normal construction, the energy in the spark is considerably greater than the minimum necessary to produce ignition. Experiments at the Bureau of Standards (Reference 2) have shown that even if the spark energy greatly exceeds this minimum value the rate of flame spread in gaseous mixtures and hence the power of the engine are unaffected. We may therefore conclude that intensity of the spark is not a measure of the effectiveness of the ignition system, and that, in general, satisfactory ignition will take place during engine operation if a spark is produced at all.

Upton (Reference 3) states that a departure of $\pm 15°$ from the best position in the timing of the spark may produce a change of 10 per cent in engine power, but that the change in power will not exceed 1 per cent provided the spark timing does not vary more than $\pm 4°$ from the optimum position. This degree of accuracy in timing is easily obtainable by a direct drive from the engine shaft to the breaker cam which determines the spark timing. It is easily possible to obtain any reasonable amount of advance and retard range on battery systems and on certain types of magnetos by shifting the position of the breaker cam or of the cam follower relative to the drive shaft. In most types of magneto, however, the cam or its follower is shifted with respect to the magnetic field also, and the requirements of the timing range constitute an important limitation on the design.

The engine speed fixes the number of sparks which the spark generator is called upon to produce per minute, and thus limits the time interval between sparks during which the energy for the succeeding spark can be stored. At high speeds this limitation of time tends to reduce the effectiveness of the spark generator either by reducing the value of current which is obtained at the instant of break, as in the case of battery systems, or by requiring in the magneto the use of a magnetic circuit giving a large number of flux reversals per revolution, and hence having available only a relatively small cross section of air gap to carry the magnetic flux. On the other hand, battery systems are able to work with full effectiveness at slow speeds while the voltage output from a magneto drops off to zero at zero speed. In certain types of magneto this difficulty is avoided by the use of impulse starters or by the device of connecting a battery in series with the magneto primary.

A spark will be produced at the spark plug only if the voltage impulse furnished by the spark generator exceeds the breakdown voltage of the gap. This breakdown voltage is affected

by a large number of variables, such as the length of the gap, the shape of the electrodes, the density of the gas mixture in the spark-plug gap, the presence of an oil film on the surface of the electrode, the temperature of the electrodes, etc. (Reference 4.)

In general, the breakdown voltage of the spark-plug gap is seldom less than 2,000 volts and seldom greater than 8,000 volts under most automotive conditions.

The leads connecting the spark generator to the spark plugs have a certain amount of capacitance, which is, of course, larger if these leads are run in a grounded metal conduit. In general, however, the capacitance of the leads is small compared with the capacitance which is inherent in the windings and the condenser of the spark generator itself; therefore the effect of such external capacitance upon the operation of the spark generator is of little importance. Nevertheless, since such capacitance is always present in the use of the spark generator, a knowledge of its effect is often desirable in order to make sure that the spark generator is not unduly sensitive to the presence of such a burden.

Since a portion of the insulator of the spark plug is liable to become covered with a conducting layer of carbon, it is very important that a spark generator be able to produce a spark even when shunted by such a conducting path. The value of the conductance (reciprocal of the shunting resistance) at which the spark generator will just fire a spark gap of standard voltage is termed by British writers the "utility" of the generator, and by some is considered as the most important property of a spark generator. In extreme cases when an exceedingly hot engine is operated with spark-plug insulators of poor quality, there may be enough conductance through the body of the insulator to affect the operation of the spark generator. In most cases, however, the conductance arises only from deposits of carbon.

From the above discussion it appears that in consideration of the electrical performance of the spark generator attention should be focused primarily on the question of whether or not it will produce the necessary sparking voltage over the needed range of conditions of shunting resistance and engine speed.

Data of this type on the various generators tested are given in section under "Experimental data."

DESCRIPTION OF THE SPARK GENERATORS STUDIED

The spark generators used in this program of measurements were selected primarily to secure as wide a variety as possible in the arrangement of the magnetic circuit. Magneto E, of foreign manufacture, was received by the bureau in 1917. Magneto K was an experimental machine submitted for test in 1917. The other systems were kindly loaned by their respective makers for the purposes of this test in 1922 and may be considered as representing the types on the market at that time.

Tables 1 and 2 give general descriptive data on these spark generators which were all of the "single-spark" type.

Magnetos A and B are supplied with jump-spark distributors, but the measurements were all made with a direct connection to the high-tension terminal.

Magneto A is of the inductor type. Both the magnet and the coils on their laminated core are stationary. The axis of the core on which the coils are wound is perpendicular to the axis of the magnetic pole pieces and to the axis of the rotor. The poles of the magnet and extensions of the core form alternate sections of magnetic material each subtending nearly 90° around the periphery of the rotor tunnel. The rotor carries two segments of laminated iron embedded in a cylindrical die casting. As the rotor revolves these segments provide a flux path of low reluctance between the magnet poles and the adjacent extension of the coil core and cause the flux through the latter to reverse its direction four times for each revolution of the rotor.

Magneto B is similar to magneto A, but its magnets have about twice the volume, and it is provided with interchangeable cams and distributors for use on either a 6-cylinder or a 12-cylinder engine.

Magneto C is of the conventional "H-armature" or shuttle type. The coils, condenser, and contact points rotate with the core and the contacts are operated by a fixed annular cam.

Magneto D has a "U-shaped magnet, mounted to rotate about its axis of symmetry and fitted with laminated pole tips. The coils are mounted on a laminated stationary core placed above the magnet and with its axis at right angles to the axis of rotation.

Magneto E is of the sleeve type. The magneto and pole pieces are similar to those of conventional H-armature type. The armature core is also of the conventional shape but is held stationary in the center of the tunnel with its magnetic axis at right angles to the magnetic axis of the magnets. In the wide air gap between the poles and the armature there revolves a hollow cylindrical sleeve. Two 90° sectors of this sleeve are of iron while the alternate sectors are non-magnetic. As the sleeve rotates through a complete revolution the flux through the armature core reverses four times. The flux through the core has a maximum value when the magnetic sectors of the sleeve overlap a pole piece on one side and the core on the other by 45°. The four positions in which this condition holds are all symmetrical and hence the maximum flux values are all equal. The positions of zero core flux, however, do not all correspond to equal geometric arrangements. In two positions the magnetic sectors are under the magnetic poles and bridge the tips of the armature; while in the other two positions the magnetic sectors lie outside the end of the core and bridge across the pole tips of the magnet. Because of this condition the alternate-current waves generated by this magneto are not quite alike, and the values of current at break as shown in Figure 35 are unequal. Since the performance data was obtained by a crest voltmeter, it corresponds to the half waves which give the greater secondary voltage (i. e., wave A at low speeds and wave B at high speeds).

Magneto F is also of the inductor type, but differs from A and E in that the axis of the stationary core is parallel to the rotor axis and lies above it. The axis of the permanent magnets is horizontal and perpendicular to the axis of rotation. The rotor tunnel is surrounded by a die casting which contains four embedded sections of laminated iron. Two of these sections lie slightly above the ends of a horizontal diameter of the tunnel and extend along its entire length. These sections form the pole faces of the magnet. The other two sections lie at the top of the casting and each is somewhat less than half as long as the rotor. These two sections form the terminal extensions of the core on which the coil is wound. Each of the sections subtends an angle of about 45°.

The rotor consists of a cylindrical die casting in which are embedded four segments of laminated iron arranged in two pairs, one at either end of the rotor. Each segment is of the same length as the smaller fixed sections which form the core terminals (i. e., somewhat less than half the rotor length), and subtends an angle of 135° on the rotor circumference. The axis of one pair of segments is at right angles to the axis of the other pair. Each revolution of the rotor causes the flux through the core to reverse its direction four times. The cam, however, is provided with only two lobes so that only/half of the possible sparks are made use of in the machine as operated. The breaker points are held open by the cam during the two quarter revolutions not used.

Magneto G is provided with an L-shaped magnet which permanently polarizes two large pole pieces. Extending from one pole piece are two cores, on one of which the coils are wound while the other or dummy core is bare. The rotation of the two-lobed rotor serves to direct the flux through one or the other of the two cores in alternation, thus providing four rather abrupt changes in the magnitude of the flux through the core for each revolution, although the flux does not reverse its direction at all. Like magneto F, however, magneto G is provided with a two-lobed cam, and thus makes use of only half the possible number of sparks.

The coils H, I, and J are wound on cores of iron wire. Coil H is of the usual open core type, having a ratio of length to diameter of 5.6: 1. I and J, however, have the external magnetic circuit closed by a yoke of iron wire so that the air gap in the magnetic circuit is only about 2 mm. long. Coils H and I are designed for use with a 6-volt battery, while coil J is designed for 12 volts.

Magneto K is of the conventional H-armature type, but has large openings cut in the solid pole pieces in order to reduce the eddy currents.

EXPERIMENTAL DATA

The following pages give in condensed form the experimental data obtained on the performance characteristics of these ignition systems.

The principal data consist of the values of maximum (or crest) secondary voltage observed with the system operating under various conditions. Figures 1 to 8 show, for the magneto system, the variation of this voltage with speed with no shunting resistance in parallel with the terminals. It will be noted that this voltage increases rapidly with speed until a value indicated by "G" is reached at which sparking occurs at the safety gap. Readings obtained at higher speeds would, of course, correspond merely to the sparking voltage of this gap and have no bearing on the functioning of the other parts of the machine. The crest voltmeter used in these measurements consisted of an electrostatic voltmeter in series with a kenetron and acted as only a very small capacitance load on the secondary terminals. (Reference 5.) When two curves are shown, one corresponds to the fully advanced and the other to the fully retarded position of the breaker mechanism.

Figures 9 to 19 show the effect of shunting resistance upon secondary voltage at full advance and at two different speeds. In the case of the magnetos the higher speed was such as to give 2,000 sparks per minute and the lower was 50 revolutions per minute. In the battery systems the speeds gave 5,000 and 800 sparks per minute, respectively. In each figure one or two curves were obtained with only the unavoidable additional capacitance caused by the leads and voltmeter. This minimum value was about 75 $\mu\mu f$. An additional curve was obtained when a condenser of about 240 $\mu\mu f$ capacitance was also connected between the secondary terminal and ground and the machine was operating at the higher speed.

The effect of capacitance is also shown in Figures 20 to 30. In these figures the curve shows the crest voltage plotted against capacitance for a speed corresponding to 2,000 sparks per minute and for a wide range of capacitance. The straight line shows the reciprocal of the square of the secondary crest voltage $\left(\dfrac{1}{V_m{}^2} \right)$ plotted against the same abscissae. The significance of the fact that this latter plot gives a nearly straight line will be discussed below.

In producing the results given above each magneto performs two fairly distinct operations: first, as a generator it produces a primary current; and second, as an induction coil it develops a high voltage when that current is suddenly interrupted. The first step in analyzing the performance, therefore, is to determine the value of the primary current flowing in each case at the instant of break, and thus separate the two parts of the operation. This was done by taking a number of oscillograms at various operating speeds. The results of such measurements are shown in Figures 31 to 39. In these measurements the oscillograph vibrator was connected in parallel with a low-resistance shunt, which in turn was inserted in series with the primary circuit. The resistance of the shunt was kept as small as possible and in most cases was about 0.07 ohm. The effect of this resistance is entirely negligible at the higher magneto speeds where the current is limited by inductance but may have caused a decrease of nearly 10 per cent in the current values at the lowest speed.

In the machines having adjustable spark timing, records were taken both at full advance and at full retard. The corresponding curves are drawn in solid lines in the figures and show the value of current at the instant the contact points begin to separate. In some cases the break at "advance" occurs before the current has reached its maximum value and the break at "retard" occurs after the current has decreased materially from its maximum value. The dotted curve marked "max" in Figures 31 and 37, shows this maximum value of current reached while the magneto was operating with the cam in the "retard" position. The maximum performance which can be obtained from a given magneto, of course, occurs with the breaker in an intermediate position, and this dotted curve enables one to estimate this performance by increasing the observed values of voltage previously given, in proportion to this increase in primary current.

In the case of system E alternate half waves are of different wave form. Two curves are therefore given in Figure 35, although this machine has fixed spark timing.
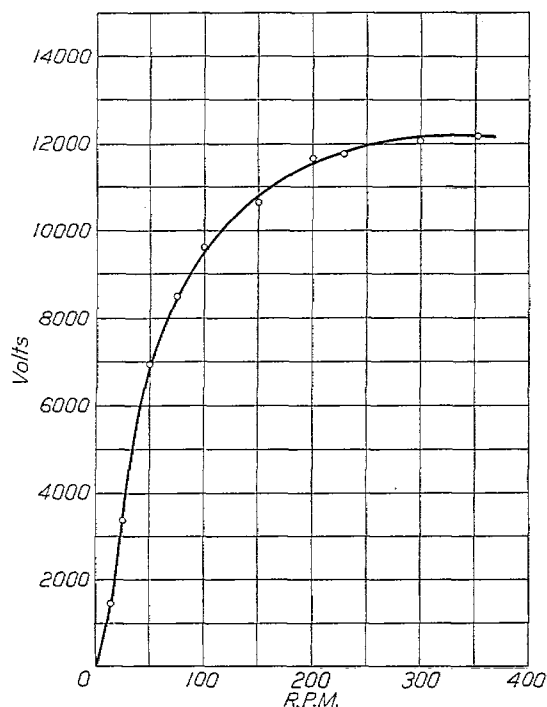
FIG. 1.—Secondary crest voltage vs. speed for magneto A (inductor type), fixed timing, 4 sparks per revolution
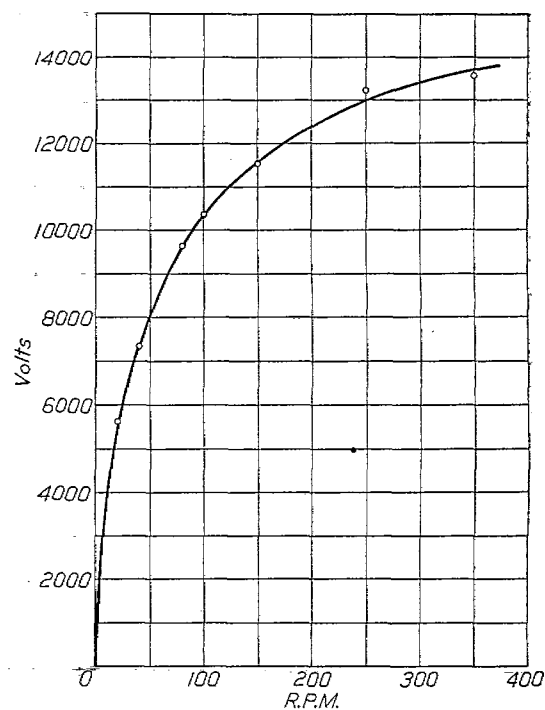
FIG. 2.—Secondary crest voltage vs. speed for magneto B (inductor type), full advance, 4 sparks per revolution
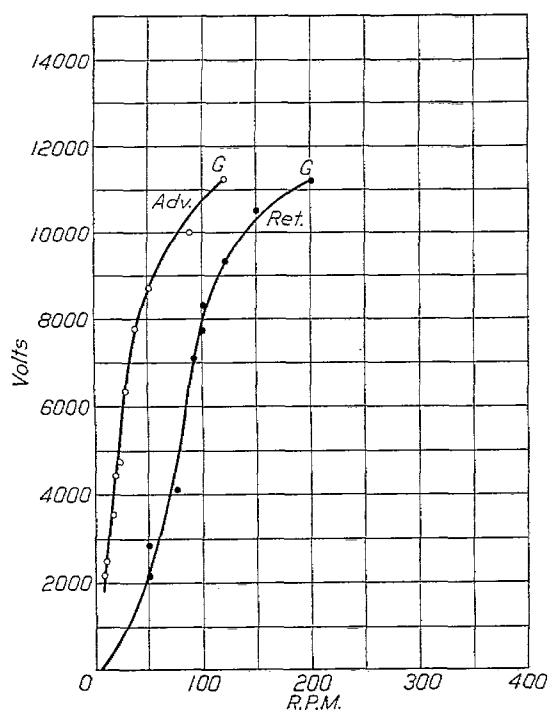
FIG. 3.—Secondary crest voltage vs. speed for magneto C (shuttle-core type) at full advance and at full retard; G indicates firing of safety gap, 2 sparks per revolution
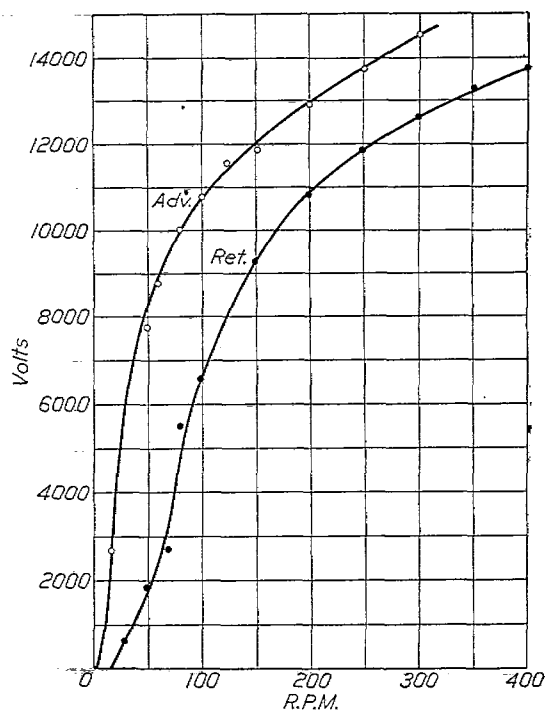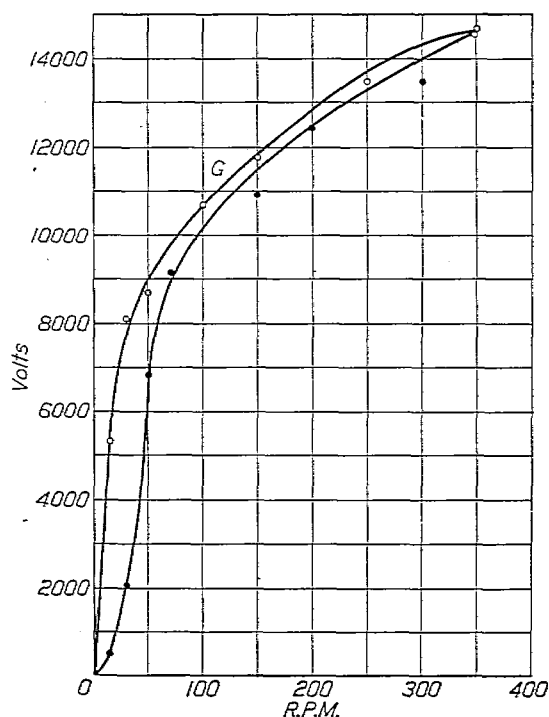
FIG. 4.—Secondary crest voltage vs. speed for magneto D (revolving-magnet type) at full advance and at full retard, 2 sparks per revolution
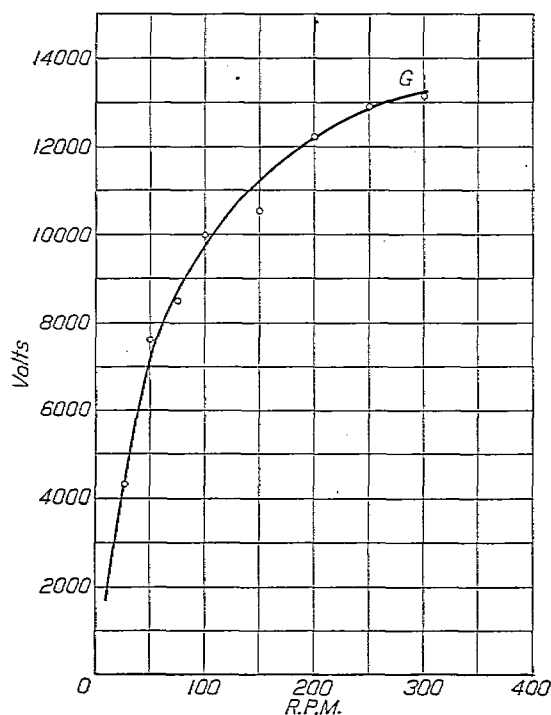
FIG. 5.— Secondary crest voltage vs. speed for magneto E (sleeve-inductor type), fixed timing; G indicates firing of safety gap, 4 sparks per revolution

FIG. 6.—Secondary crest voltage vs. speed for magneto F (inductor type) at full advance and at full retard; G indicates occasional firing in safety gap, 2 sparks per revolution
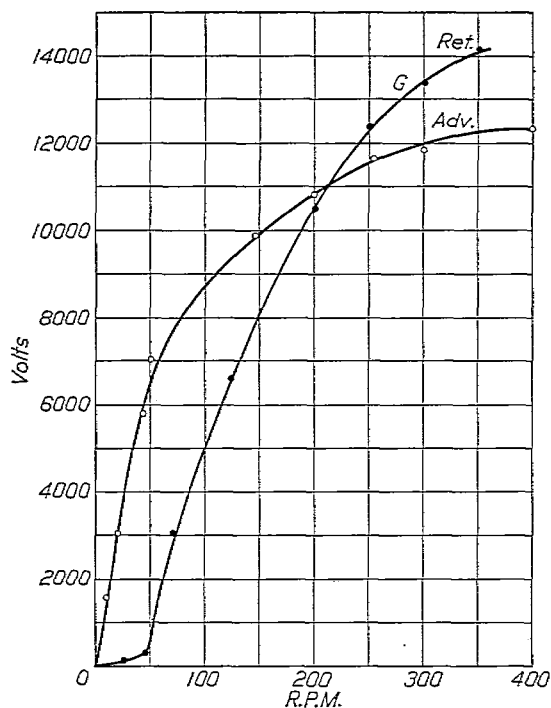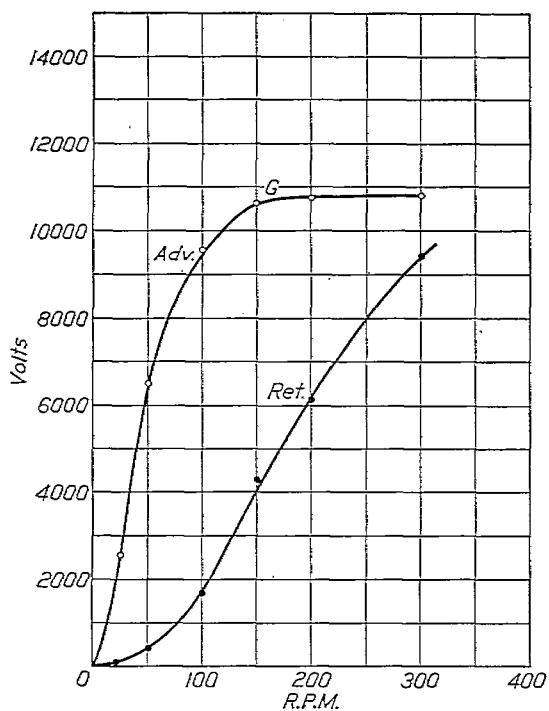

F IG. 7.—Secondary crest voltage vs. speed for magneto G (pulsating-flux type) at full advance and at full retard; G indicates firing at safety gap, 2 sparks per revolution

FIG. 8.—Secondary crest voltage vs. speed for magneto K (shuttle-core type) at full advance and at full retard; G indicates firing at safety gap, 2 sparks per revolution
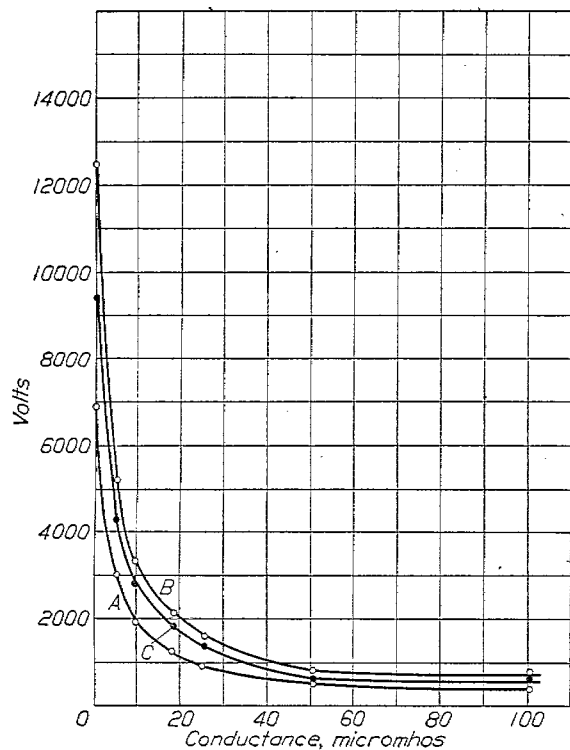
FIG. 9.—Secondary crest voltage vs. shunting conductance for magneto A (inductor type); A at 50 R. P. M., B at 500 R. P. M., C same as B but with an additional condenser of 250 μμf capacitance shunting the secondary
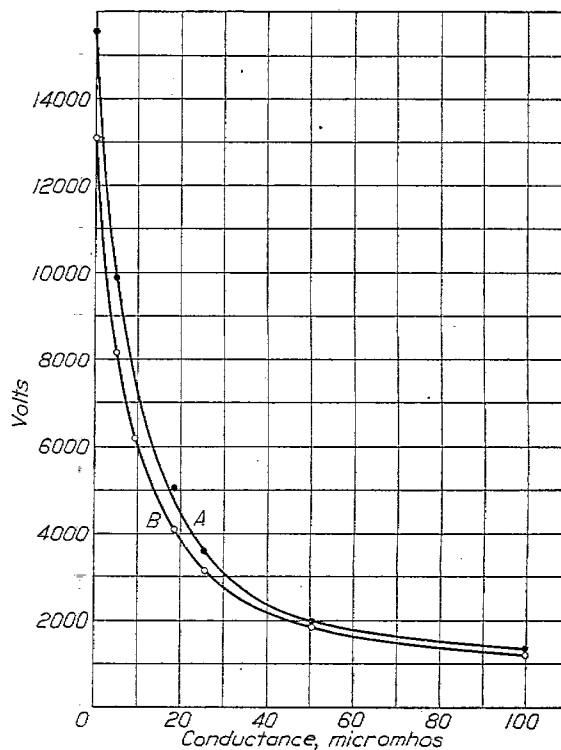

FIG. 10.—Secondary crest voltage vs. shunting conductance for magneto B (inductor type) at full advance; A at 500 R. P. M., B same as A but with an additional condenser of 260 μμf capacitance shunting the secondary
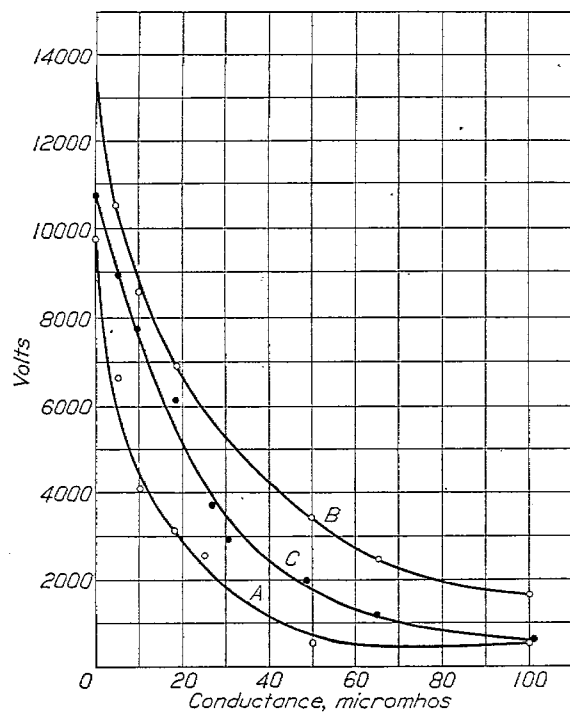

FIG. 11.—Secondary crest voltage vs. shunting conductance for magneto C (shuttle-core type) at full advance; A at 50 R. P. M., B at 1,000 R. P. M., C same as B but with additional condenser of 230 μμf capacitance shunting the secondary
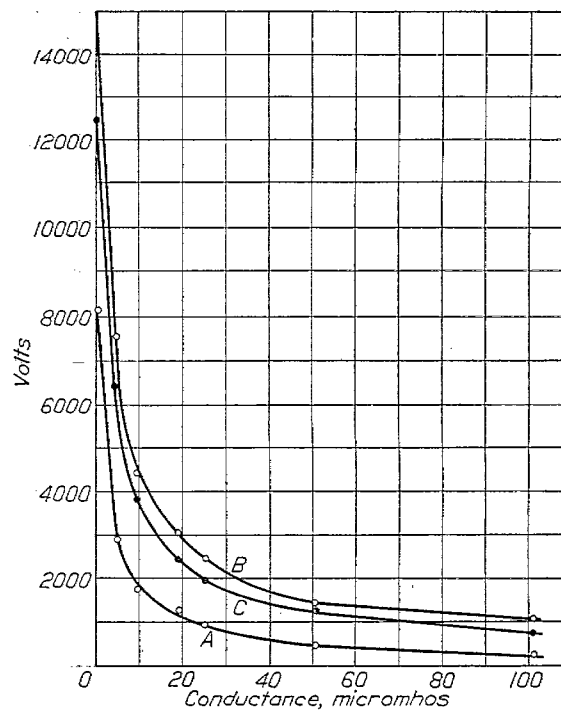

FIG. 12.—Secondary crest voltage vs. shunting conductance for magneto D (revolving-magnet type); A at 50 R. P. M., B at 1,000 R. P. M., C same as B but with an additional condenser of 280 μμ capacitance shunting the secondary
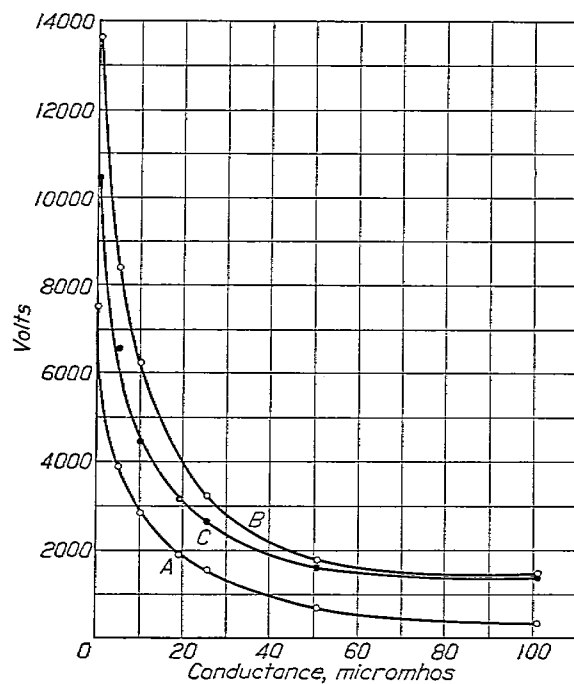
FIG. 13.—Secondary crest voltage vs. shunting conductance for magneto E (sleeve-inductor type); A at 50 R. P. M., B at 500 R. P. M., C same as B but with an additional condenser of 250 $\mu\mu$f capacitance shunting the secondary
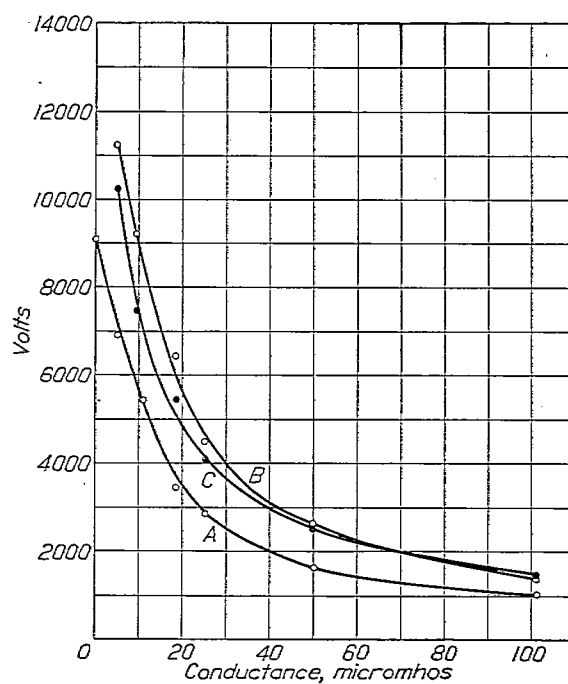

FIG. 14.—Secondary crest voltage vs. shunting conductance for magneto F (inductor type) at full advance; A at 50 R. P. M., B at 1,000 R. P. M., C same as B but with an additional condenser at 240 $\mu\mu$ capacitance shunting the secondary
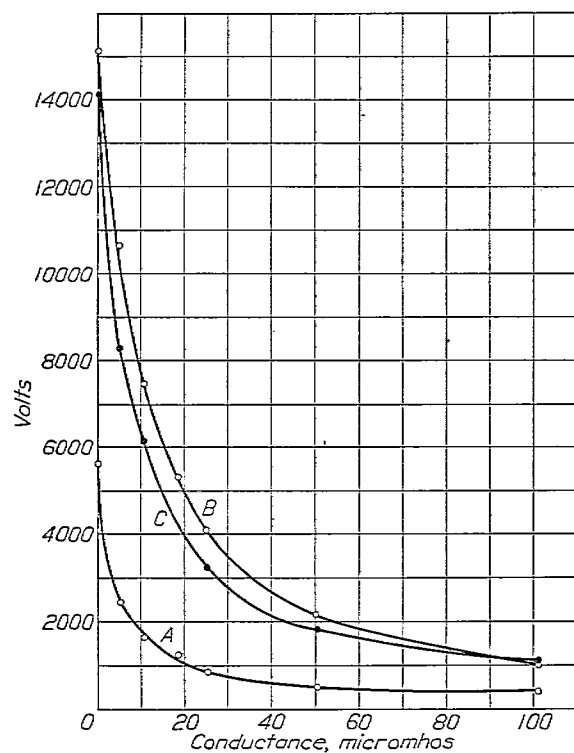

FIG. 15.—Secondary crest voltage vs. shunting conductance for magneto G (pulsating-flux type); A at 50 R. P. M. at full advance, B at 1,000 R. P. M. at full retard, C same as B but with additional condenser of 200 $\mu\mu$f capacitance shunting the secondary
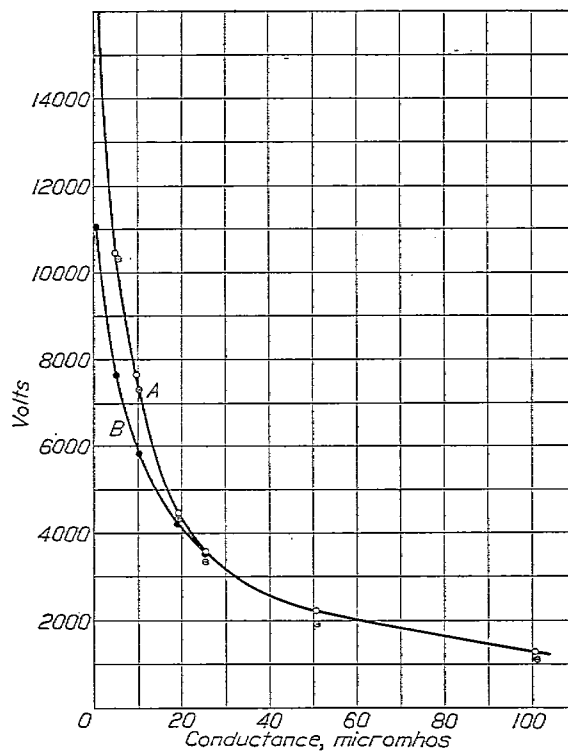

FIG. 16.—Secondary crest voltage vs. shunting conductance for 6-volt coil H; A at 800 sparks per minute, B same with an additional condenser of 330 $\mu\mu$f shunting the secondary; circles with dot indicate values observed at 5,000 sparks per minute without the condenser
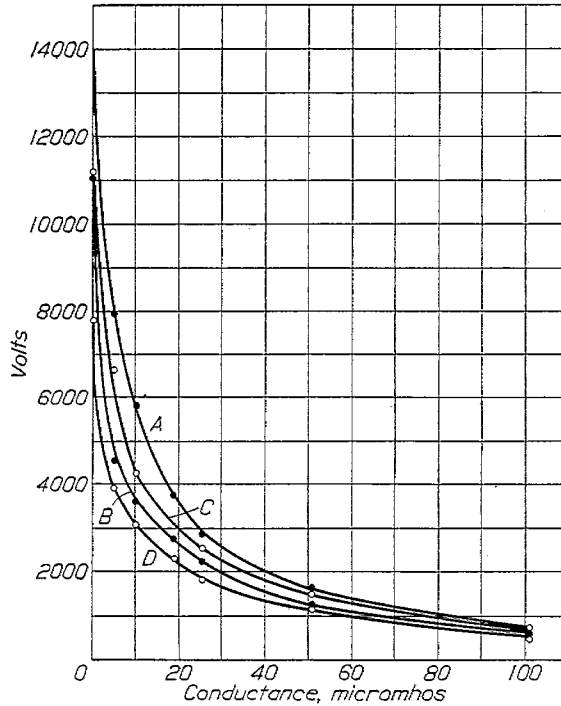
FIG. 17.—Secondary crest voltage vs. shunting conductance for 6-volt coil I; A at 800 sparks per minute, B at 5,000 sparks per minute, C same as A but with a condenser of 330 μμf capacitance shunting secondary, D same as B but with a condenser of 330 μμf capacitance shunting the secondary

FIG. 18.—Secondary crest voltage vs. shunting conductance for 12-volt coil J; A at 800 sparks per minute, B at 5,000 sparks per minute, C same as A but with an additional condenser of 330 μμf capacitance shunting the secondary, D same as B but with an additional condenser of 330 μμf capacitance shunting the secondary

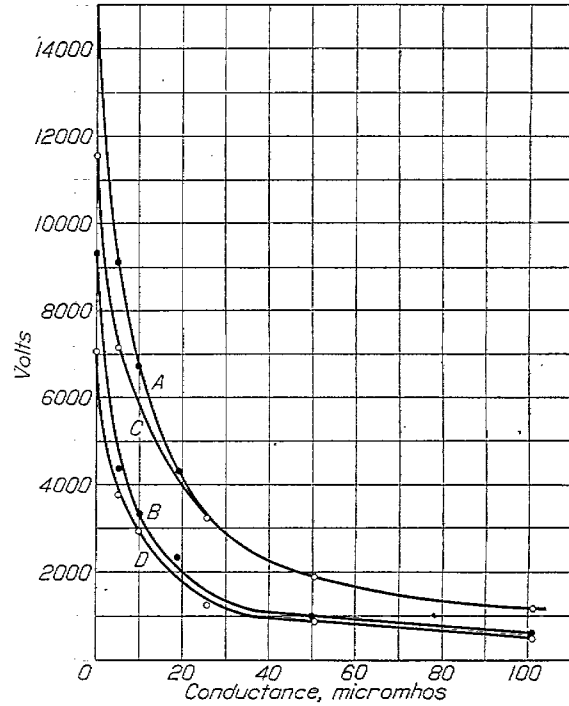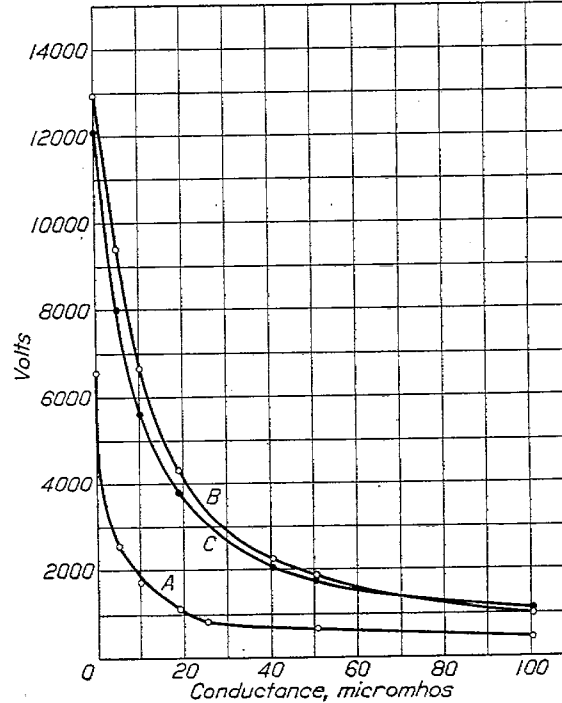FIG. 19.—Secondary crest voltage vs. shunting conductance for magneto K (shuttle-core type) at full advance; A at 50 R. P. M., B at 1,000 R. P. M., C same as B but with an additional condenser of 240 μμf capacitance shunting the secondary
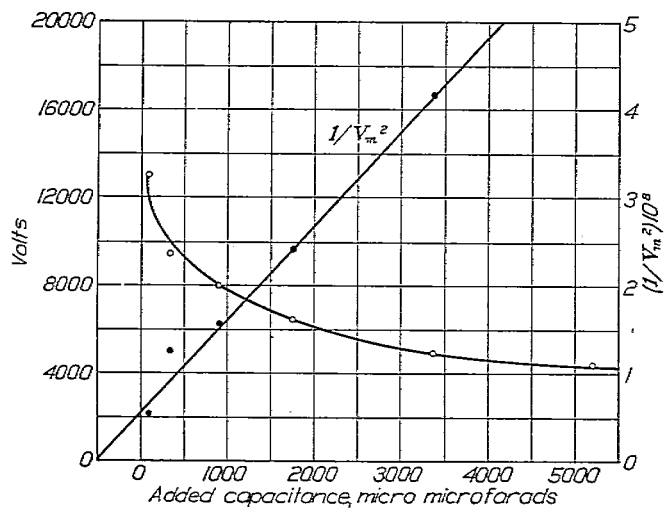
FIG 20.—Secondary crest voltage vs. shunting capacitance for magneto A (inductor type) fixed timing, 500 R. P. M. The straight l ine is a graph of $1/V_m^2$ vs. capacitance
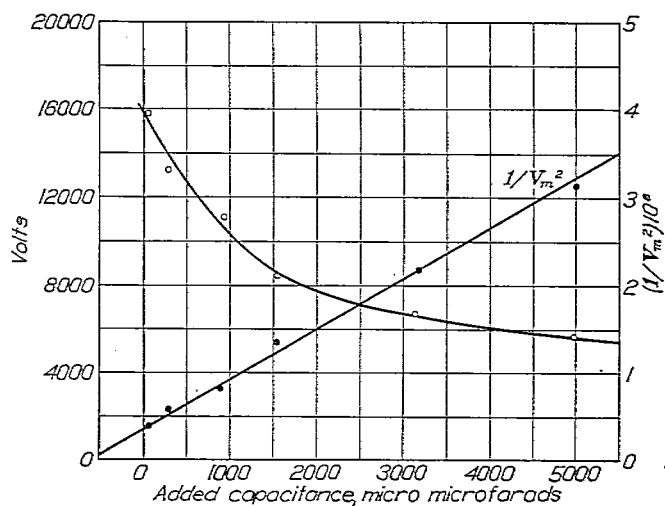
FIG. 21.—Secondary crest voltage vs. shunting capacitance for magneto B (inductor type) at full advance, 500 R. P. M. The straight line is a graph of $1/V_m^2$ vs. capacitance

FIG. 22.—Secondary crest voltage vs. shunting capacitance for magneto C (shuttle-core type) at full advance, 1,000 R. P. M.
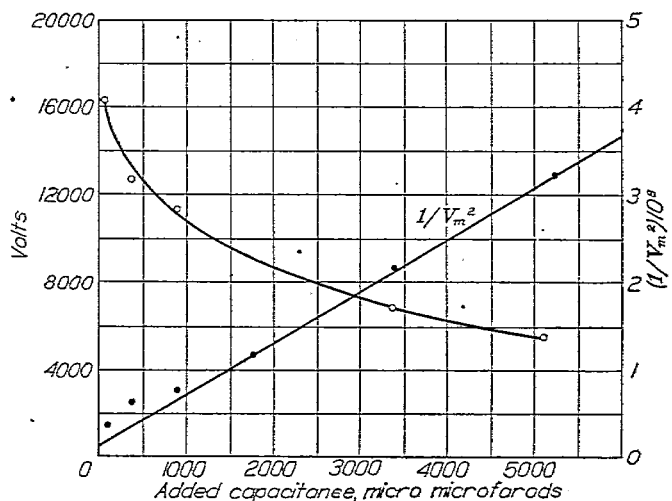
FIG. 23.—Secondary crest voltage vs. shunting capacitance for magneto D (revolving-magnet type) at full advance, 1,000 R. P. M. The straight line is a graph of $1/V_m^2$ vs. capacitance
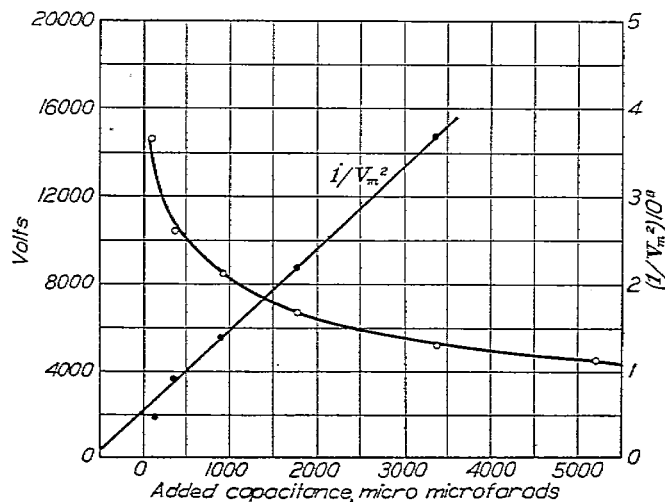
FIG. 24.—Secondary crest voltage vs. shunting capacitance for magneto E (sleeve-inductor type), fixed timing, at 500 R. P. M.
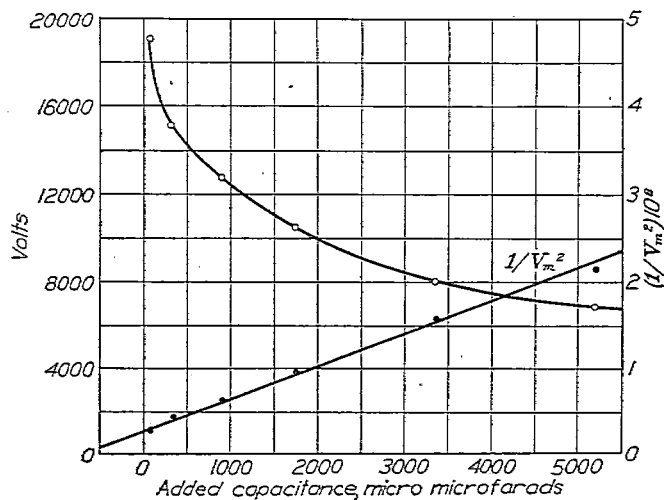
FIG. 25.—Secondary crest voltage vs. shunting capacitance for magneto F (inductor type) at full advance, 1,000 R. P. M.
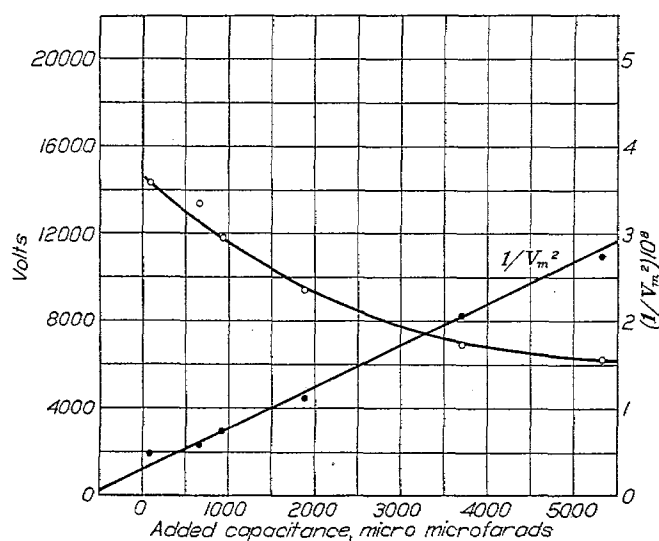
FIG. 26.—Secondary crest voltage vs. shunting capacitance for magneto G (pulsating-flux type) at 1,000 R. P. M. at full retard. The straight line is a graph of $1/V_m^2$ vs. capacitance
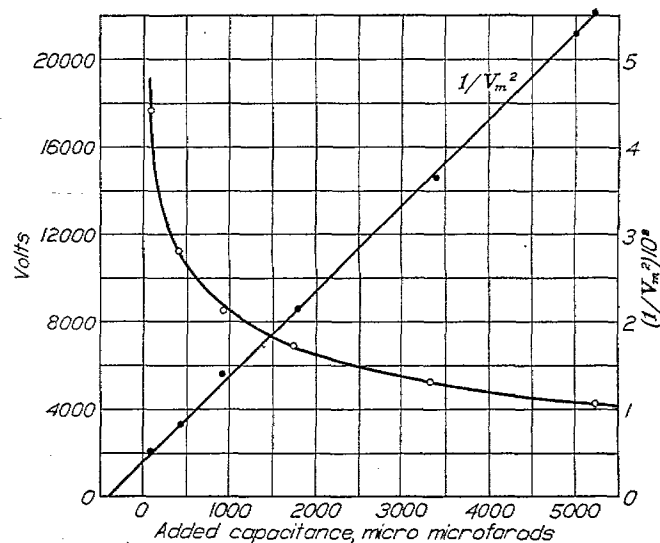
FIG. 27.—Secondary crest voltage vs. shunting capacitance for 6-volt coil H at 800 sparks per minute. The straight line is a graph of $1/V_m^2$ vs. capacitance
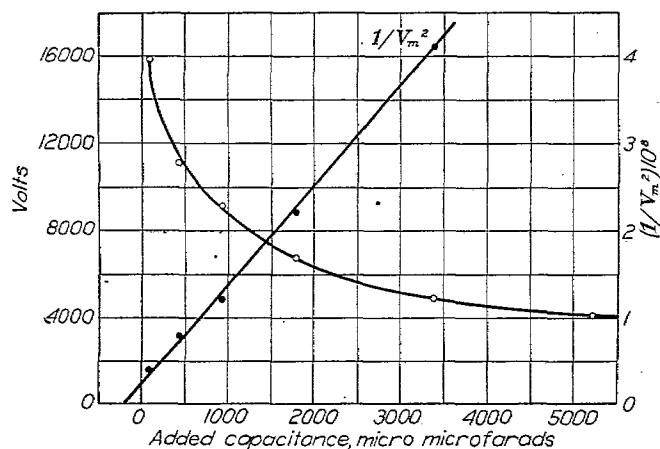
FIG. 28.—Secondary crest voltage vs. shunting capacitance for 6-volt coil I at 800 sparks per minute. The straight line is a graph of $1/V_m^2$ vs. capacitance
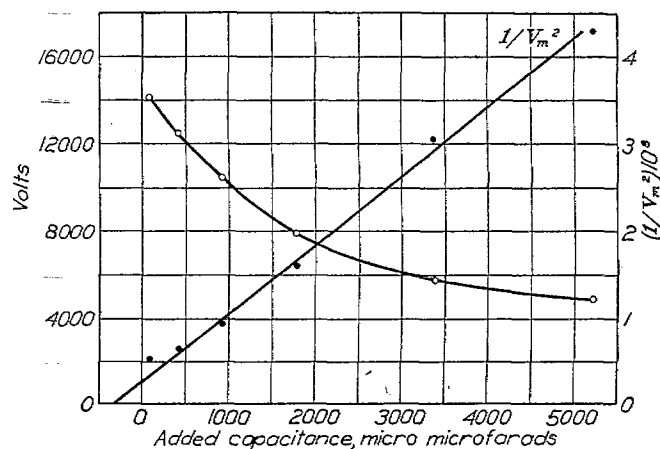
FIG. 29.—Secondary crest voltage vs. shunting capacitance for 12-volt coil J at 800 sparks per minute. The straight line is a graph of $1/V_m^2$ vs. capacitance
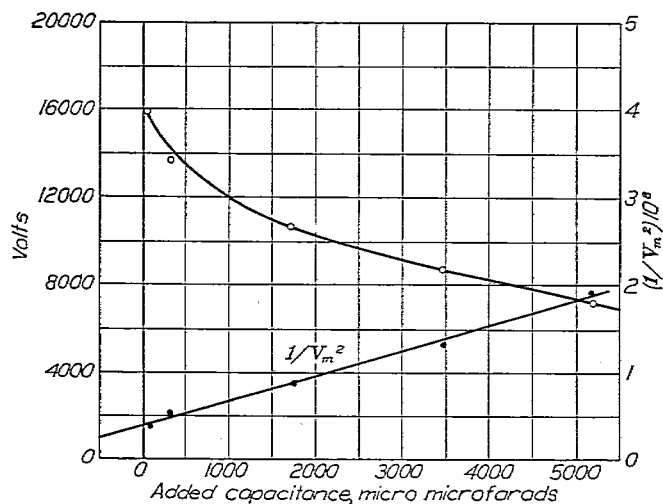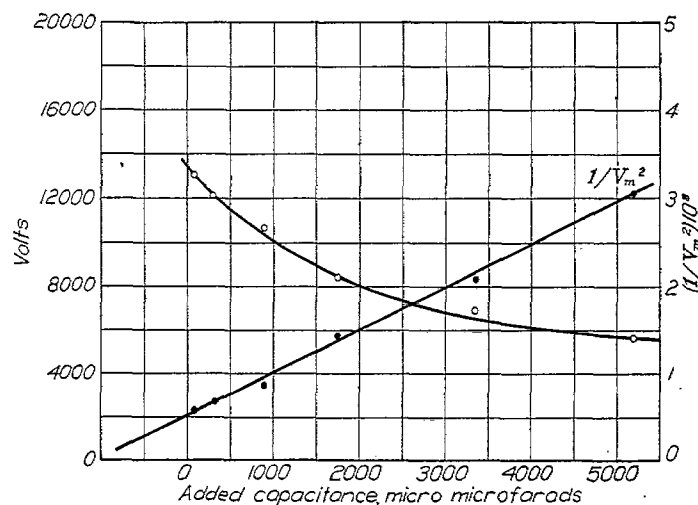

FIG. 30.—Secondary crest voltage vs. shunting capacitance for magneto K (shuttle-core type) at full advance, 1,000 R. P. M.
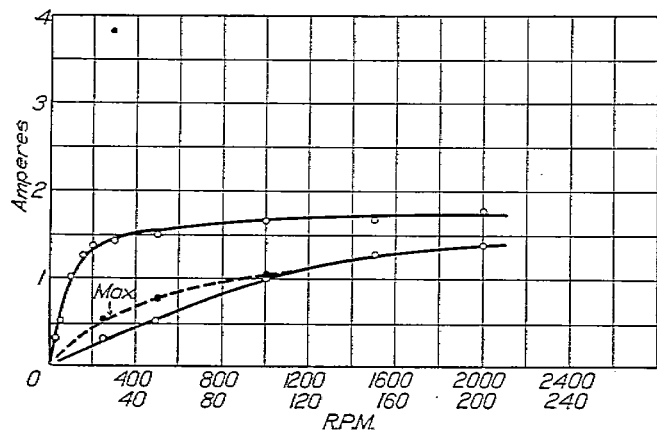
FIG. 31.—Primary current at break vs. speed for magneto A (inductor type), fixed timing. Lower curves show low-speed values to a larger scale of speed. Dotted curve shows maximum value of current which occurred before break at low speeds
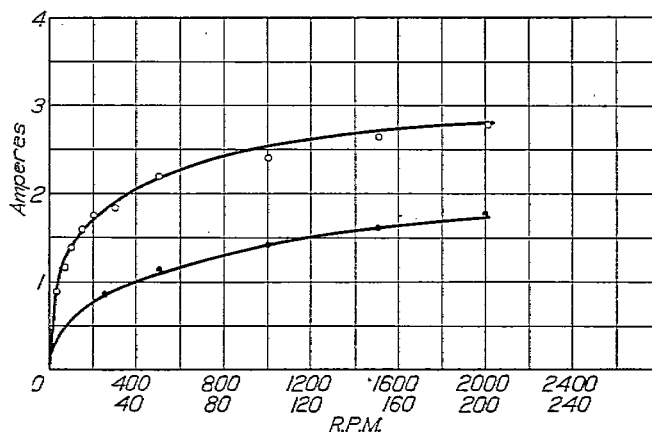
FIG. 32.—Primary current at break vs. speed for magneto B (inductor type) at full advance. Lower curve shows low-speed values to a larger scale of speed
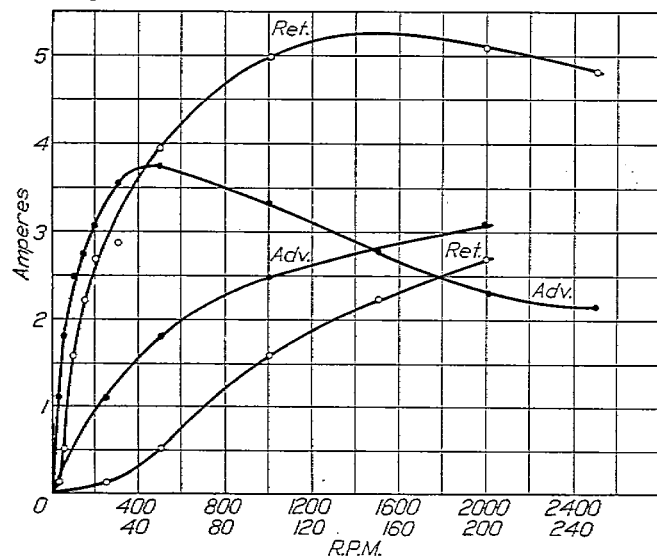
FIG. 33.—Primary current at break vs. speed for magneto C (shuttle-core type). Lower curves show low-speed values to a larger scale of speed
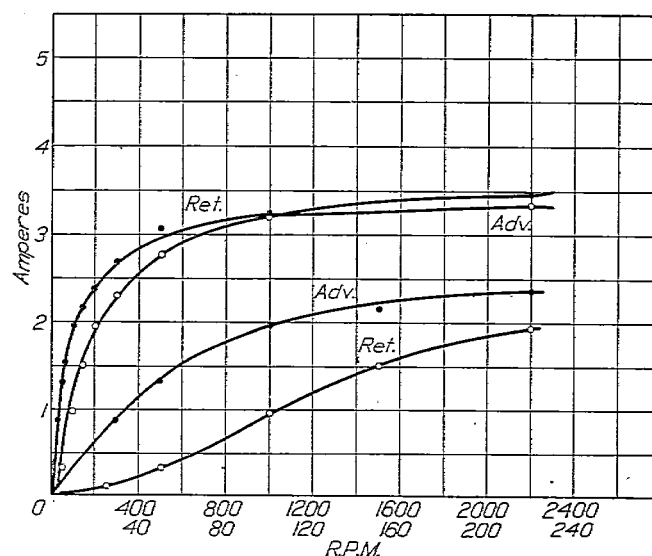
FIG. 34.—Primary current at break vs. speed for magneto D (revolving-magnet type). Lower curves show low-speed values to a larger scale of speed
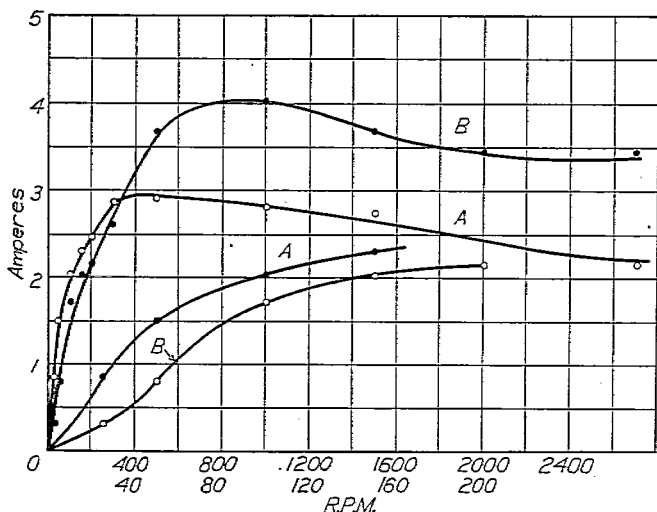
FIG. 35.—Primary current at break vs. speed for magneto E I(sleeve-inductor type), fixed timing. Alternate waves differ. Crest of wave A occurs later with respect to "break" than that of wave B
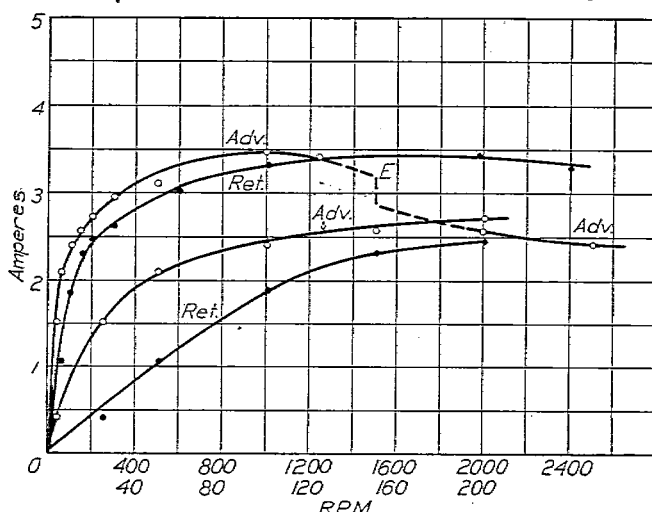
FIG. 36.—Primary current at break vs. speed for magneto F (inductor type). Lower curves show low-speed values to a larger scale of speed. Break in "advanced" curve at E is caused by occurrence of an "extra" spark at high speed which interferes with building up of current for the following regular spark

In the case of the coils I and J, the curves shown in Figure 38 were obtained by computation as follows: An oscillogram taken at slow speed on each coil gave a record of the rise of current with time. Points were scaled from these oscillograms and the quantity $\log \frac{I}{I_0}$, where I_0 is the final steady value of current was plotted as ordinate against the time at which the current had the value I as abscissa. The resulting graph was in all cases very closely a
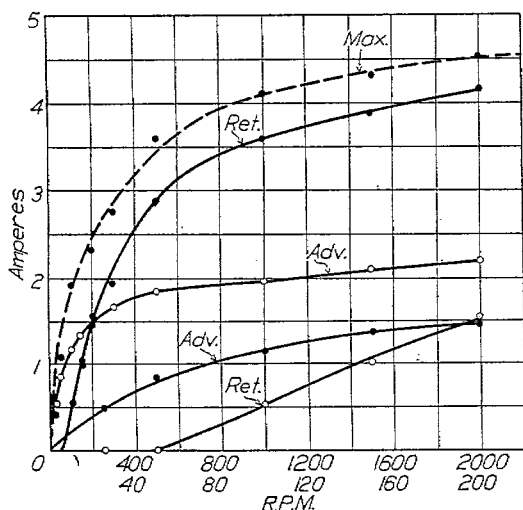
FIG. 37.—Primary current at break vs. speed for magneto G (pulsating-flux type). Lower curves show low-speed values to a larger scale of speed. Dotted curve shows crest value of current wave when operating at full retard
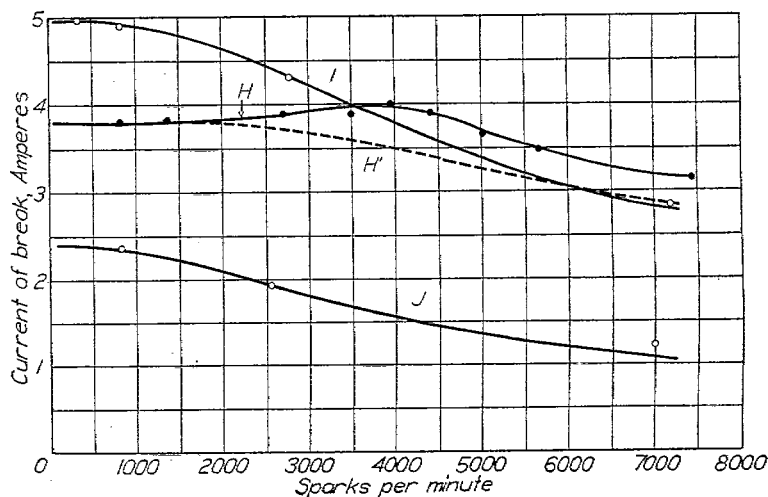
FIG. 38.—Primary current at break vs. speed in sparks per minute for coils: H (6-volt), I (6-volt), and J (12-volt). The rise in curve H results from action of ballast resistor coil, and the dotted curve H' shows the values which would result if the resistance of the circuit remained constant
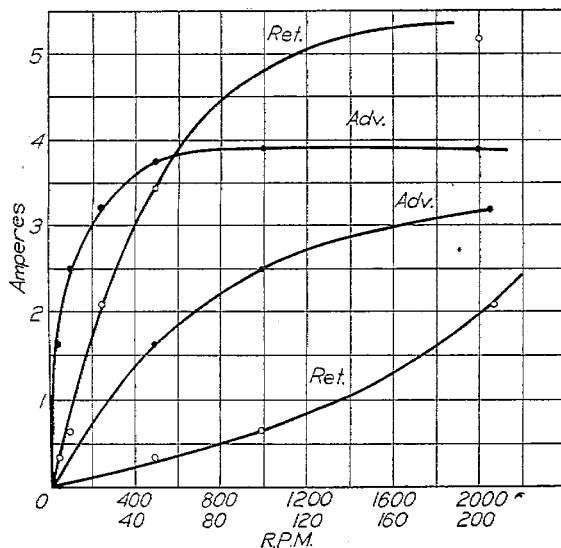
FIG. 39.—Primary current at break vs. speed for magneto K (shuttle-core type). Lower curves show low-speed values to a larger scale of speed

straight line indicating that the inductance of the circuit was practically constant. The time constant $\frac{L_1}{R_1}$ of the circuit can be computed from the slope of this line and is given in column 18 of Table 2. The currents at break for various cam speeds were then computed from the equation

$$I = I_0\left(1 - e^{\frac{-R_1\,at_0}{L_1}}\right) \tag{1}$$

When t_0 = time interval between sparks.

a = fraction of time that the breaker is closed.

$\frac{L_1}{R_1}$ = time-constant of circuit.

$I_0 = \frac{E}{R_1}$ = final current at low speeds.

The points indicated by the solid circles in Figure 38 show values obtained directly by oscillograms taken at the corresponding speeds and serve to verify the correctness of the plotted curves.

System H was provided with a ballast resistor of material having a high-temperature coefficient of resistance. The main object of such a resistor is to limit the amount of current which would flow if the engine should stop with the breaker points in contact, and thus avoid overheating the primary winding of the spark coil. However, the presence of this resistor has the further effect of changing the rate at which the primary current falls off with increasing engine speed as is shown by a comparison of curves H and H' of Figure 38. The former (solid)

curve shows the values of current at break actually observed with the oscillograph, while the latter (dotted) curve shows the values which would result if the resistance and inductance of the circuit had remained constant at the different speeds. An analysis of a typical oscillogram showed that even in this system the growth of current was quite closely in accordance with the simple exponential law, and hence that the ballast resistor did not change appreciably in temperature or resistance during the course of a single cycle, although these values shift materially when the engine speed is altered to a new value.

Auxiliary measurements were also made on the voltage generated when the magnetos were rotated on open circuit. It was found that both the crest value and the effective (root-mean-square) value of primary voltage were quite closely proportional to the speed of rotation. In columns 10 and 11 of Table 1 are given the effective and crest voltage for a speed of 1,000 R. P. M., and in column 12 the quotient of these values. Since the ratio of crest to effective value for a sine wave is only 1.41, whereas in these magnetos values as high as 4.0 were obtained, it will be seen how very peaked the magneto waves are.

As a basis for a further analysis of the performance of the spark generators, measurements were made of the flux turns linking the secondary winding for various angular positions of the armature and for various values of primary current at each position. (Reference 6.) By divid-
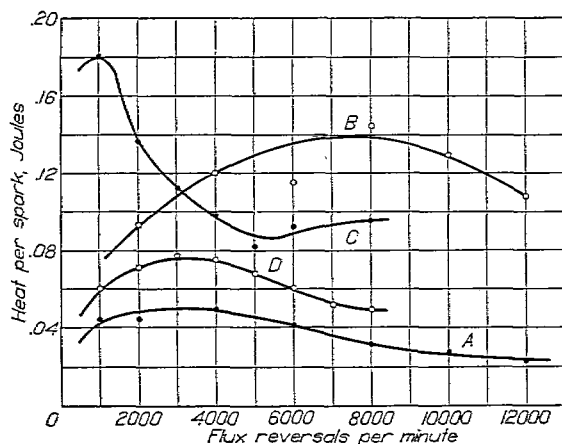
FIG. 40.—Heat energy (in joules) disspiated in spark gap vs. speed (in flux reversals per minute) for systems A, B, C, D, operating at full advance
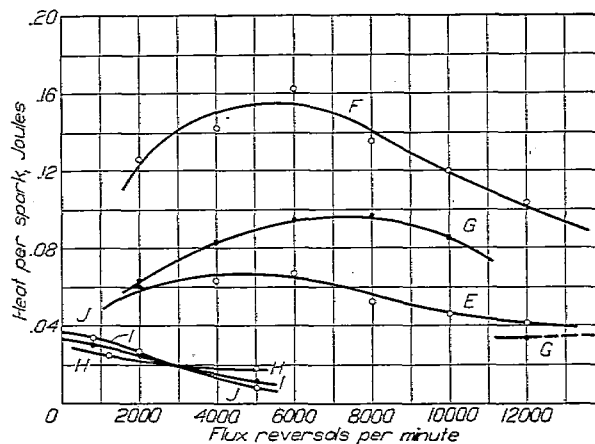
FIG. 41.—Heat energy (in joules) dissipated in spark gap vs. speed (in flux changes per minute) for systems E, F, G, H, I, and J, operating at full advance. The break in curve G results from serious arcing at the breaker points

ing the change in flux turns between any two conditions by the corresponding change in current, a value is obtained for the inductance of the circuit, and values thus obtained are given in columns 9 and 10 of Table 2.

The area between a graph of flux turns vs. current and the axis of flux turns also gives the energy change occurring between the two conditions indicated by the ends of the graph. The figures given in column 9 of Table 3 are values thus obtained for the maximum possible energy which could be transformed and delivered to the spark gap by an ideal magneto having the same magnetic circuit as the actual machine but free from all sources of energy loss such as resistance and eddy currents. Column 8 indicates the corresponding values of current at break which would be attained. While these are limiting figures, unattainable in practice, they nevertheless form a useful standard against which to compare the actual performance. It was, however, impracticable in most cases to carry the measurements to the full current value given in column 8 and these data are therefore uncertain to the extent of this extrapolation.

The figures in column 10 which indicate the energy per spark available at the instant of break when the generator is operating at 2,000 sparks per minute at full advance were obtained by combining the flux-meter data with the values of current at break found by the oscillograph.

The figures in column 11 similarly give the energy available when operating at 50 R. P. M., full advance.

The actual heat energy liberated in the spark gap was also measured on each system at several speeds by causing the spark to occur inside a hollow copper block (Reference 7) which served as a calorimeter. The spark occurred between blunt nickel electrodes spaced 2.1 mm. apart. The results of these measurements are plotted in Figures 40 and 41. The ordinates give the energy in joules per spark (1 joule = 0.24 calories = 1 watt-second) and the abscissæ the speed of the spark generator expressed as flux reversals (or changes) per minute.

A considerable number of other supplementary measurements were made to give the necessary data for a detailed study of the cause of the observed characteristics. The results are given in the tables.

The ratio of turns and the coupling coefficient were obtained with an accuracy of better than 1 per cent by the null method previously described by one of the authors. (Reference 8.) The actual number of turns could be estimated only approximately from measurements made by means of an exploring coil of a known number of turns wound over the regular windings. The flux turns linking this coil were compared with those linking the secondary winding by an opposition method similar to that used for the ratio measurement. This comparison was made for flux changes caused in two ways: (a) by energizing an external electromagnet applied to the extremities of the core; and (b) by sending current through the primary winding. A considera-tion of the probable flux paths in the two cases shows that the apparent number of secondary turns is too small in case (a) and too large in case (b). The mean value is given in column 3 of Table 2. Column 2 gives the corresponding number of primary turns.

In the best case the difference between the upper and lower limits thus obtained was only 2.5 per cent, while in the worst case it was 48 per cent. In the case of system F winding data were kindly supplied by the manufacturer, and the experimental values were found to agree with these to 1 per cent.

An attempt was made to obtain a quantitative basis for estimating the effects of eddy currents during the abrupt flux changes occurring in the normal operation of these spark gen-erators by observing the corresponding effects produced when the generators were subjected to harmonically alternating flux changes of various frequencies. For this purpose the secondary circuit of each system was connected in one arm of a bridge circuit supplied with alternating current. (Reference 9.) A number of frequencies from 25 cycles to 3,000 cycles per second were used, and at each frequency the apparent resistance and inductance of the winding were measured. Also the capacitance between the high-tension terminal of the secondary and the frame or core was determined by balancing a fifth bridge arm, consisting of a variable condenser and resistance connected between the frame of the magneto and the opposite supply terminal of the bridge. The voltage applied to the winding was kept proportional to the frequency and was 230 volts per 1,000 cycles, so that all the observations on any one system were made at practically the same flux density. The decrease in inductance with increase of frequency which was observed can therefore be properly attributed to eddy currents. In columns 12, 13, and 11 of Table 2 there are given the effective inductances and resistances of the secondary windings at 3,000 cycles per second and the corresponding inductance at zero frequency as found by extrapolating the observed curve. These values correspond to the fully advanced position of the breaker, and have been corrected for the effect of the internal capacitance of the winding. The difference between their values and those in columns 9 and 10 of Table 2 arises from the different flux density at which the magnetic circuit was working. From the decrease in inductance and the increase in resistance it is possible to estimate for any frequency the time constant T_e of the eddy current circuit and the coupling coefficient k^2_e by which it is coupled magnetically to the windings. These values are given in columns 8 and 9 of Table 5.

In order to obtain a value for the internal capacitance C_w (Reference 10) of the windings, which is needed to correct the alternating-current bridge data, a series of capacitance measure-ments were made at radio-frequencies in the range from 40 to 300 kilocycles. It was found that most of the coils showed a change of about 15 $\mu\mu$f in effective capacitance at about 100 kilocycles. Presumably this is the result of a local resonance point in the winding, which cuts out part of the possible capacitance at the higher frequencies. Consequently the larger value

corresponding to lower frequencies was used in later computations and is given in column 5 of Table 4.

The value of the terminal capacitance C_t as observed with the alternating-current bridge is given in column 6. The capacitances of the primary condensers were measured directly by a microfarad meter with the results given in column 2. Combining these values according to the relation

$$C_o = \frac{C_1}{n^2} + C_t + \frac{4}{3}\,C_w \qquad (2)$$

gives the total effective capacitance of the system referred to the secondary side and the values thus obtained are given in column 7 of Table 4. The factor $\frac{4}{3}$ enters because in operation there is a uniform voltage gradient along the winding while in the measurements at radio-frequency the voltage distribution being determined solely by capacitances is such as to minimize the capacitance. The capacitance (C_g) from the inner layer of the winding to the core is given in column 4, but is of importance only in the case of two-spark magnetos.

DISCUSSION OF RESULTS

As previously indicated, the most important electrical performance characteristic of a spark generator is the secondary crest voltage at the instant of break, V_m. This voltage depends upon the primary current at break I_b and the values of shunting resistance S, and capacitance C_a, which may be connected in parallel with the secondary. An examination of the observed data shows that there are certain theoretical and empirical relationships between these quantities and the electrical constants which are useful in the comparison of spark generators and in predicting the behavior of a given spark generator under various conditions.

The first relation is that between the maximum induced voltage and the primary current at break. As can be seen from Figures 1 to 8, in the magneto systems the observed crest voltage increases with speed until at a speed of about 200 R. P. M. it reaches such a high value that sparks are produced at the safety gap. For higher speeds the observed voltage is merely the sparking voltage of the gap and bears no direct relation to the magneto. For speeds less than this value, however, there is a very definite and simple relation between the crest voltage V_m, and the current at break I_b. From the simple theory of the magneto, it would be expected that (Reference 11)

$$V_m = \frac{I_b}{n} F \sqrt{\frac{L_2}{C_o}} + E_r \qquad (3)$$

where L_2 and C_o are the inductance and capacitance of the equivalent single-coil model and F is a factor resulting from the damping effect of the resistance and eddy currents. E_r is the electromotive force acting in the secondary winding as the result of the rotation of the armature at the instant of maximum voltage. When the magneto is operating with its breaker retarded E_r has decreased to nearly zero before the breaker opens and may therefore be neglected. At advance, however, the crest of the induced voltage occurs while an appreciable fraction of the rotational E. M. F. is still acting. Nevertheless, since in the speed range which is here of interest both E_r and I_b are nearly proportional to the speed, it would be expected that V_m would be proportional to I_b. This relation was tested for the various magnetos where data were available over a considerable range of current values and the proportionality was found to hold within limits of ± 6 per cent in most cases and ± 12 per cent in all but one case. The ratio V_m/I_b may be called the "impulsive impedance" of the windings and denoted by the letter Z_m. Values of this quantity referred to the secondary side for the several systems operating at full advance are given in column 15 of Table 2.

From the value of L_2 and C_o for corresponding conditions given in column 10, Table 2, and column 7, Table 4, the factor $Z_2 = \sqrt{\frac{L_2}{C_o}}$ can be computed with the result given in column 14, Table 2. Comparing these figures with those in column 15 shows that the factor F must

have the values given in column 16 to account for the losses and eddy current effects. The frequency of oscillation of a circuit having these values of inductance and capacitance is given in column 17, Table 2. The actual frequency of the oscillations occurring immediately after "break" is probably materially higher than this because of the effects of eddy currents in reducing the effective inductance.

The relation between secondary crest voltage V_m and shunting resistance S, as shown by the curves of Figures 9 to 19, is less readily determined on theoretical grounds. At very large values of S the crest voltage approaches the limiting value of $I_b Z_m$ or $\dfrac{I_b Z_2 F}{n}$ and becomes independent of S. If the magnetic coupling between the two windings of the magneto or coil were perfect (Reference 12) so that M was exactly equal to $\sqrt{L_1 L_2}$, then for very low values of S the crest voltage would approach the value $V_m = \dfrac{I_b S}{n}$. However, in actual spark generators as shown by the data in columns 5 and 6 of Table 2, the coupling although close, is not perfect. It can be shown by theoretical considerations that in such cases, if the primary resistance is small, the current in the primary winding will oscillate and the maximum secondary voltage will be produced when the currents in the primary and secondary circuits are flowing in opposite directions. In such a case the crest voltage approaches the value $V_m = \dfrac{2 I_b S}{n}$ as the damping effects become small.

For values of S intermediate between these two limiting conditions even the simplest forms of theoretically equivalent circuit lead to very complicated expressions for the relation between V_m and S. However, the simple empirical equation

$$V_m = \frac{2 I_b S Z}{n(2S + Z)} \tag{4}$$

has been found to fit the observations fairly closely, where Z is to be regarded as an empirical constant which has the dimensions of an impedance, and becomes identical with nZ_m if the empirical equation fits exactly when the secondary circuit is open.

Fig. 42.—Solid lines are graphs showing the applicability of the empirical equation

$$V_m = \frac{2 I_b S Z}{n(2S + Z)}$$

for the effect of shunting resistance (S) on the secondary crest voltage (V_m). Abscissas are values of S. Ordinates are corresponding values of S/V_m. If the formula were exact, these lines should be straight, the intercept should be $n/2I_b$, and the slope should be $n/I_b Z$. Solid circles show observed values on magneto C at 50 R. P. M., full retard; magneto E at 500 R. P. M.; magneto F at 50 R. P. M., full advance; coil H at 800 sparks per minute; coil J at 5,000 sparks per minute. Dotted lines show the same graph as determined by values of I_b, n, and Z, measured separately

The easiest test of this equation is obtained by plotting the quantity $\dfrac{S}{V_m}$ as ordinate against S as abscissa. If the above equation holds, the result should be a straight line as appears from rearranging equation (4) to give

$$\frac{S}{V_m} = \frac{n}{I_b Z} S + \frac{n}{2 I_b} \tag{4a}$$

Such plots for a few of the systems studied are given in Figure 42. In the case of other systems (as, for instance, D) the graphs showed a very definite curvature, and it must therefore be concluded that equation (4) is only a rough approximation in some cases.

If the empirical equation (4) really represented the facts over the whole range, then the intercept on the axis of S/V_m of the graphs of S/V_m vs. S should have the value of $\frac{n}{2\,I_b}$. This relation was found to obtain in many of the cases tested. In other cases V_m was 20 to 30 per cent less than this relation would indicate. This is presumably the result of an appreciable damping of the oscillation; still other cases showed values of V_m higher than the theoretical. These can only be accounted for by stating that in these generators the equation does not fit the facts closely enough to justify extrapolation to extremely low values of S.

The slope of the line obtained by plotting S/V_m vs. S has the value $\frac{n}{I_b Z}$ and hence the quotient of twice the intercept divided by the slope of the line equals Z, and should theoretically be equal to $n\, Z_m$ or $F\, Z_2$.

This relation was found to be only approximately true. The points marked by open circles in Figure 42 were located by using the value of $\frac{I_b}{n}$ obtained by the oscillograph and the value of Z_m obtained as the mean ratio of crest voltage to current at break at the lower speeds. In the cases plotted and in a few others the agreement between these two sets of data obtained from independent observations is quite satisfactory. On the other hand, in several cases the directly observed values of Z_m were nearly 60 per cent in excess of those deduced from the S/V_m vs. S lines. The disagreement in the intercept values in no case exceeded 30 per cent. In general, with any given system, a change such as adding capacitance in parallel with the secondary which decreases Z_2 is also found to decrease the slope of the S/V_m vs. S line but to leave its intercept unchanged. A change such as speed which changes I_b, is found to markedly change the intercept of the line, but to affect only slightly the quotient of slope to intercept.

The relation between crest voltage and capacitance added in parallel with the secondary is indicated by the equation

$$V_m = \frac{I_b}{n}\, F\sqrt{\frac{L_2}{C_o + C_a}} + E_r \qquad (5)$$

This is the same as equation (3) except that the total effective capacitance now consists of two parts, C_o, which represents that inherent in the spark generator; and C_a, which may be added in the form of the capacitance of the spark plug cables or of condensers. If E_r were zero and F a constant, then a plot of $\frac{1}{V_m^2}$ as ordinate against C_a as abscissa would yield a straight line. The intercept of this line on the axis of abscissæ would give C_o and the slope of the line would be $\frac{1}{F^2 I_b^2 L_2}$. Unfortunately, F varies when different condensers C_a are connected, because the frequencies of the resulting oscillations are changed. Also in most magnetos the E.M.F. of rotation E_r is not entirely negligible. It happens, however, that in all the systems tested the effects of F and E_r were such that the plot of $1/V_m^2$ vs. C_a was almost a straight line, though slightly convex upward. This empirical straight line relation can therefore be used with some assurance to predict the variation of V_m with C_a in other systems. (See figs. 20 to 30.) The intercept of the plotted lines, however, was in all but one case decidedly greater than the value of C_o obtained by other methods, and was often two or three times that value.

While the preceding discussion has shown certain relations between performance and other measurements on a given spark generator, a correlation of the performance data with the energy and current data given in columns 8 to 12 of Table 3, for the different generators, yields considerable additional information as regards two of the desirable properties of a spark generator, viz, (1) its ability to produce a reasonably high voltage on open circuit under adverse conditions, such as low speed when the plug is fouled with oil; and (2) its ability to fire a plug which is fouled with carbon. For the former property we may consider that the maximum secondary voltage developed at 50 R. P. M., as given in column 3 of Table 5, is representative. Combining this value with the total effective capacitance of the system (referred to the secondary side) which is given in column 7 of Table 4, we get the amount of energy (given in column 6 of Table 5)

which the system actually has delivered into its capacitance at the instant of maximum voltage. Column 4, on the other hand, gives the energy which was apparently available at the instant of break, as indicated by the current determined by the oscillograph and the inductance determined by the flux meter. A comparison of columns 4 and 6 shows a very low efficiency as indicated by the figures in column 7, which are the quotients obtained by dividing the numbers in column 6 by those in column 4. These show that in one case less than one-tenth and in all but one case less than four-tenths of the energy originally at hand appears in the secondary at the time when it is most wanted to raise the voltage at the plug electrodes. If, however, the spark gap is so short that a spark can easily be produced, we find that the energy then delivered into it has the values [2] shown by the figures in column 5. Strangely enough these values are much greater than those in column 6 and thus show that there must be some process occurring while the voltage is building up which ties up much of the original energy in unavailable form, but which will release at least part of it later to be dissipated as heat in the spark gap. While rotational energy may account for some of the excess of column 5 over column 6 in the case of
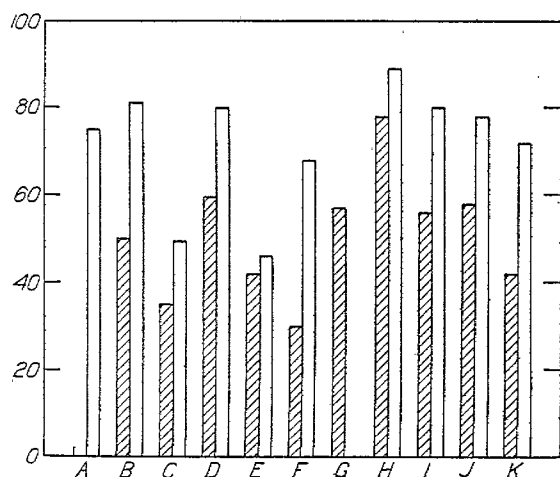

FIG. 43.—Diagram showing the observed and computed voltage efficiencies of the system when operating at 50 R. P. M. The 100 per cent line indicates the voltage to be expected if all the energy stored magnetically was used without losses to develop voltage. The heights of the shaded blocks indicate observed crest voltages in per cent of this value. The heights of the open blocks indicate the crest voltages computed on the assumption that the only losses present are those resulting from an eddy-current circuit such as would account for the measured inductance and resistance at 3,000 cycles

the magnetos, it can not do so in the battery systems, and it can not account for the great difference between column 4 and column 6 since it was not included in the computation of either energy value. An estimate of the possible energy losses in the resistance of the windings during the time the voltage is building up shows them to be negligible, and we must therefore attribute the low efficiency to some other cause. Eddy currents induced in the core, pole faces, and other parts of the magnetic circuit seem to be the principal cause of this poor performance.

An independent and roughly quantitative estimate of the effects to be expected from eddy currents can be obtained from alternating-current bridge measurements, by a rather involved process which will be treated in another paper. From measurements of this kind made with 3,000-cycle alternating current, an estimate was made of the crest voltage to be expected with eddy currents flowing, as compared to that which would result in the absence of eddy currents. The results are shown by Figure 43. In this figure the heights of the shaded blocks show the actual crest voltage at 50 R. P. M. on a scale such that the 100 per cent line corresponds to the voltage which would be produced if all the energy available at the instant of "break" were effective in charging the capacitance of the system. The heights of the open blocks in Figure 43 show to the same scale the crest voltage computed theoretically from the alternating-current bridge measurements. It will be noted that the theoretical and actual departures from the ideal of 100 per cent are of the same order of magnitude. The departures from exact agreement can be accounted for, at least in part, by the fact that in actual operation the flux density in the magnetic circuit was much higher than could be used during the alternating-current measurements. Consequently the permeability was higher, and the eddy currents were of considerably greater relative magnitude. Any other source of energy loss, such, for example, as sparking at the breaker contacts would also tend to lower the actual voltage below the theoretical value.

For the second important property of a spark generator (i. e., ability to fire a plug which is fouled with a conducting carbon deposit), we may take 5,000 volts as a typical operating voltage

---

[2] These latter values were obtained by interpolation of the data plotted in figs. 40 and 41 on the assumption that the curves were straight line between the origin and the first plotted point. This assumption is, of course, not true but insures that the values given in column 5 are certainly less than the correct values.

and from the curves plotted in Figures 9 to 19 read off the greatest value of the shunting conductance or "utility" which may be connected in parallel with the spark plug without causing the generator to fail to produce this voltage. Values thus obtained are given in column 2 of Table 6, and column 3 gives the reciprocal of the utility, i. e., the lowest possible shunting resistance. Column 4 gives the product of the conductance by the assumed voltage (5,000 volts), and hence is the value of the current flowing through the secondary winding and the resistor at the instant of maximum voltage. A comparison of these values with those in column 5, which gives the quotient of primary current at break divided by the ratio of turns, shows the former to exceed the latter in all but two cases. Column 6 is the quotient of column 4 divided by column 5. The fact that the secondary ampere turns thus exceed, and are often nearly double, the initial primary ampere turns, indicates that at the instant of maximum secondary voltage the primary current has reversed its direction and tends to demagnetize the core, while the secondary current has risen to such a value as to neutralize the primary ampere-turns and, in addition, to maintain much of the original magnetic flux.

Any actual spark generator presents such a complex electrical system as to defy a rigorous mathematical analysis of its performance. Certain simplified model circuits have been suggested which serve to imitate with more or less fidelity the principal features of the actual machine. (Reference 13.) Of these the simplest is the "single-coil model," which consists of a single inductance coil connected in parallel with a condenser and the breaker terminals. This model will account for the relations between crest voltage and current at break, and between crest voltage and shunting capacitance, which are discussed above. The "closed-coil model" adds to the single-coil model an extra circuit, the currents in which tend to simulate the eddy currents in the actual magneto. The open blocks in Figure 43 were computed by the use of this arrangement of circuits, and it would seem to be useful in connection with problems of design in which eddy-current effects are to be considered. Neither of these models, however, correctly represents the conditions of current flow described in the preceding paragraph, which occurs when the secondary terminals are heavily shunted. The more complex "double-coil model" must, therefore, be used in discussing these phenomena. This model consists of two inductively coupled circuits, each containing a coil and a condenser.

FIG. 44.—Diagram comparing the observed and computed crest values of current, with the current at break, when the systems are operating at 1,000 R. P. M. with a shunting resistance sufficient to reduce the crest voltage to 5,000 volts. The horizontal line marked "1" indicates the primary current at break referred to the secondary side. The heights of the shaded blocks indicate the observed crest values of secondary current expressed as fractions of the current at break. The heights of the open blocks indicate the same quantity as computed from the coupling, inductance, capacitance, and shunting resistance. The horizontal line marked "2" indicates the values to be expected if the primary current had reversed its direction without loss

A complete theory of this model has been worked out by Taylor-Jones (Reference 14), but the application of it is very laborious. For the case where a low resistance is connected across the secondary condenser it is possible to work out some rather simpler relations by making two simplifying assumptions. (Reference 6.) The first is that the secondary capacitance is absent. This assumption should not introduce serious errors for low values of shunting resistance, since the time required for currents to adjust themselves between the secondary capacitance and the resistance then becomes very short compared to the period of the other oscillations concerned. The second assumption is that the effective resistance of the primary winding is zero. This assumption is entirely justifiable as regards the resistance of the copper coil itself. It can not, however, be taken for certain a priori that the energy loss resulting from eddy currents is negligible under these conditions. However, the figures given in column 7 were computed on this assumption, and it will be noted that they do not differ very greatly from the observed values in column 4. The comparison of theory and observation in this respect is also shown by Figure 44. Here the open blocks show the
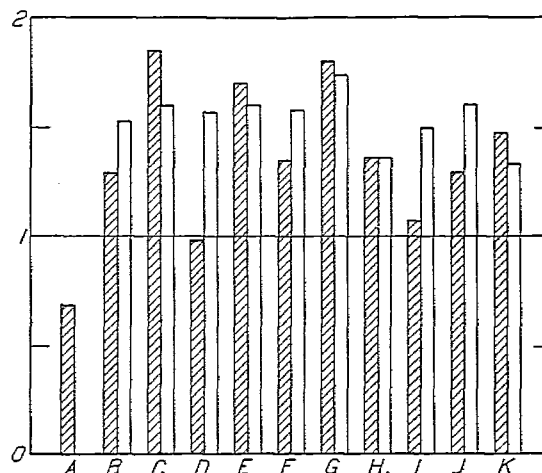
theoretical performance (i. e., crest value of secondary current expressed in terms of the current at break), while the shaded blocks show the observed performance. The letters indicate the ignition system to which each pair of blocks corresponds. The horizontal line marked "1" indicates the value of current at break (referred to the secondary side), and it will be noted that in most cases the observed crest value rises to nearly double this amount. It will be seen that most of the observed values are less than the computed, and such departures can be readily attributed to the effect of eddy-current loss in increasing the effective primary resistance. These departures are relatively small and indicate that the effect of eddy currents is much less important on this property of a spark generator than it is on the open-circuit voltage. The abnormally high value observed with system C can only be attributed to experimental error.

An inspection of the values of total stored magnetic energy given in column 10 or of the heat per spark actually delivered, as given in column 12 of Table 3, shows a very noticeable difference between the values for the magnetos and for the battery systems. That this difference is not a fortuitous result of the particular systems selected for this study but is a necessary result of the relatively low voltage of the batteries available in battery ignition systems, can be seen from the following considerations. For a battery system supplying an engine at a given speed there is available a certain fixed time t_o (which can not be greater than the interval between sparks) in which to store magnetic energy. The current at break in such a system is

$$I_b = \frac{E}{R_1}\left(1 - e^{\frac{-R_1 t_0}{L_1}}\right)$$ (6)

and the stored energy is

$$W_b = \frac{L_1 I_b^2}{2} = \frac{E^2 L_1}{2 R_1^2}\left(1 - e^{\frac{-R_1 t_0}{L_1}}\right)^2$$ (7)

For a coil of a given shape and size a change in the number of primary turns will change both R_1 and L_1 in the same ratio and leave the time constant $\frac{L_1}{R_1}$ unaffected. A change in the size of the entire structure, however, will both increase L_1 and decrease R_1. The energy may therefore conveniently be expressed in terms of the time constant $T=\frac{L_1}{R_1}$ as

$$W_b = \frac{E^2 T}{2 R_1}\left(1 - e^{\frac{-t_0}{T}}\right)^2$$ (8)

In this form it appears that as the size of the coil is increased the value of W_b will at first increase but that beyond a certain size the effect of the T in the exponent of the last term will more than offset the gain in the first factor. There is, therefore, for a given circuit resistance a certain best value of T, and hence a best size of coil which will store the greatest amount of energy. This best value of T is approximately equal to 0.79 t_o.

As the resistance is decreased the energy will increase in inverse proportion. However, the designer is limited by the fact that the breaker contact can reliably interrupt the current only if it is less than a certain fairly definite value, which we may call I_c, and which in practice seems to be less than 5 amperes. Since this value should not be exceeded even at low engine speeds, the resistance can not be made less than E/I_c, so that the maximum energy attainable at the full rated speed is

$$W_m = \frac{E I_c t_o\ 0.79}{2}\left(1 - e^{-1.27}\right)^2$$ (9)

$$= 0.20\ E I_c\ t_o$$

and at slow speeds the energy is 0.394 $E I_c\ t_o$.

Considerations of convenience in the number of cells to be carried usually limits the battery voltage to 6 or 12 volts. A magneto, on the other hand, operating at normal speeds, may generate in its primary a crest voltage of about 100 volts, and hence can store 10 to 20 times as much energy during the interval between sparks.

SUMMARY AND CONCLUSIONS

In the work here reported the performance of a series of spark generators of various types has been studied under various conditions of operation and their electrical and magnetic characteristics have been determined.

Certain theoretical and empirical relationships were correlated with the measured properties, and it was found that these relationships can be made to serve a useful purpose in the analysis and comparison of the behavior of various types of spark generator under various conditions.

It would appear also that a careful consideration of the characteristics and performance data here presented in the light of certain simplified models should lead to improvements in design.

If one regards the problem of automotive ignition as a whole, it appears that at present the burden of operation is divided between the spark plug and the spark generator in such a way that the plug is required to maintain two conditions: First, the sparking voltage between its electrodes must lie in the range of from 1,000 to 8,000 volts. A voltage below the lower limit may give a spark too feeble for ignition and a voltage above the upper limit may not always be attainable by the spark generator. This requirement can be easily met by a plug of good design. Secondly, the shunting resistance in parallel with the spark gap must be greater than about 50,000 ohms. It is not at all easy to satisfy this second requirement under conditions of low temperature and closed throttle with a plug which also must not cause preignition when the engine is operating at full power. One may, therefore, conclude that any improvement in the design of spark generators which will directly or indirectly increase their "utility" and permit of operating a spark plug with a heavier carbon deposit than at present will, to the same extent, relieve the burden which has hitherto fallen upon the shoulders of the long-suffering spark plug.

Regarded solely from the point of view of the energy values involved, it appears that there is much room for improvement both (1) in the voltage developed with a clean plug at low speeds or low battery voltage; and (2) in the "utility" when operating with dirty plugs. In the former case the net unavoidable energy expenditure required to produce the observed voltage is in many cases only one-third to one-tenth of that initially stored in the magnetic system. In the latter case there is also required the additional amount of energy which is dissipated in the carbon layer from the instant when the secondary voltage starts to rise until it reaches the sparking voltage of the gap. The total energy requirement for a 5,000-volt gap shunted with the resistances given in column 3 of Table 6 is given in column 10 of Table 6 and is seen to be much smaller than the initial stored energy given in column 11.

The cause of this obvious ineffectiveness of spark generators of the types here studied is fundamentally the same in both cases. A parasitic circuit magnetically coupled to the primary circuit temporarily checks the flux changes and ties up in unavailable form much of the initial store of energy until the moment of maximum voltage has passed; only to release it later when it merely serves to overheat and disintegrate the spark-plug electrodes. When the plug is clean the parasitic circuit is in the body of the iron core and pole pieces of the magnetic circuit. When the plug is dirty the principal parasitic current flows through the secondary winding and the carbon deposit.

Several modifications of the conventional systems are in use which may considerably improve their electrical performance under certain conditions. Among these are the use of an auxiliary spark gap in series with the spark plug, the connection of a battery in series with the primary winding of a magneto, and the impulse starter. If a valid theoretical basis for ignition system design can be built up, then it should be possible to so shift the design as to transfer the benefit derived from any such modification, or from such changes as the use of finer laminations or of steels of higher resistivity, to the condition where the gain is most needed. The double-coil model of Armagnat (Reference 15) and Taylor-Jones (Reference 16) and the simpler but less complete single-coil and closed-coil models suggested by one of the present authors (Reference 17) are steps toward such a basic theory.

The present work has shown that, so far as the measurements here made are concerned, the single-coil model gives a substantially correct picture of the operation of the spark generator with the secondary circuit open. The factor F which is introduced to cover the various energy losses is found to range from 0.31 to 0.75 in the systems tested. The closed-coil model is doubtless a closer approximation to the actual condition of affairs and the data show that the insertion into the equations of this model of the values for the constants of the eddy current circuit determined by alternating-current bridge measurements gives a fair approximation to the observed results.

When the secondary circuit is closed through a shunting resistance of low value, however, the single-coil model ceases to represent the facts even qualitatively and recourse must be made to the more complex double-coil model. This latter can, however, in this case, be simplified materially by omitting the secondary condenser without leading to very wide departures from observed results. Observations on the crest value of the voltage across the primary winding also indicates that the double-coil model and not the single-coil model should be used in considering problems such as the voltage stress imposed on the primary condenser and the contact points.

The connection between these models and the actual spark generators as regards details of design such as numbers of turns, core dimensions, etc., are not covered by the program of measurements here presented and must await the results of further work on specially constructed systems in which only one design constant is varied at a time.

NOTATION

a = fraction of time breaker contacts are closed.

C = capacitance.

C_a = capacitance added in parallel with the secondary.

C_g = capacitance from ground terminal of winding to frame. .

C_w = capacitance distributed through layers of the secondary winding.

C_0 = total effective capacitance of system under normal conditions referred to the secondary.

C_1 = capacitance of primary condenser.

E = voltage of battery.

E_r = E. M. F. of rotation.

$e = 2.718$ = base of Napierian logarithms.

F = factor by which crest voltage is reduced as a result of eddy current and resistance losses between instants of break and of crest voltage.

I = current.

I_b = current in primary at instant of break.

I_c = greatest value of current which contacts can break satisfactorily.

$I_0 = \dfrac{E}{P}$ = final steady value of current in battery-coil system.

$k^2 = \dfrac{M^2}{L_1 L_2}$ = coefficient of coupling between primary and secondary circuits.

k^2_e = coefficient of coupling between eddy-current circuit and winding (in the closed-coil model).

L = self-inductance.

L_1 = inductance of primary winding.

L_2 = inductance of secondary winding. .

M = mutual inductance.

n = effective turn ratio.

R_1 = resistance of primary circuit.

S = resistance of leakage path shunting the secondary.

$T = \dfrac{L_1}{R_1}$ = time constant of primary winding.

T_e = time constant of eddy current circuit.

t = time.

t_o = time interval between successive sparks.

V_m = crest value of voltage at secondary.

W = energy in spark.

W_b = stored magnetic energy at instant of break.

W_m = maximum value of W_b.

Z = empirical constant in equation 4 which has the physical dimensions of a resistance.

$Z_m = \dfrac{V_m}{I_b}$ = "impulsive impedance."

$Z_2 = \sqrt{\dfrac{L_2}{C_o}} = \dfrac{nZ_m}{F}$ = theoretical impulsive impedance referred to the secondary.

REFERENCES

1. C. C. Paterson and N. R. Campbell: Some Characteristics of the Spark Discharge and Its Effects in Igniting Explosive Mixtures. Physical Soc. Proc. (London), 31, p. 168; 1919.

2. D. W. Randolph and F. B. Silsbee: Flame Speed and Spark Intensity. N. A. C. A. Technical Report No. 187; 1924.

3. G. B. Upton: Spark Advance. Automotive Industries, 49, pp. 14 and 76; 1923.

4. F. B. Silsbee: The Sparking Voltage of Spark Plugs. N. A. C. A. Technical Report No. 202; 1925.

5. C. H. Sharp and E. D. Doyle: Trans. A. I. E. E., 35, p. 99; 1916. C. C. Paterson and N. R. Campbell: Phil. Mag., 37, p. 301; 1919.

6. F. B. Silsbee and D. W. Randolph: The Linkage Current Diagram for Representing Magneto Performance. Bureau of Standards Scientific Paper in preparation. (Containing the details of this method and a more complete discussion of the results.)

7. F. B. Silsbee, L. B. Loeb, and E. L. Fonseca: Heat Energy of Various Ignition Sparks. N. A. C. A. Technical Report No. 56; 1920. (Containing a detailed description of the method used.)

8. F. B. Silsbee: Characteristics of High-Tension Magnetos: Part II. N. A. C. A. Technical Report No. 58; 1920.

9. F. B. Silsbee: The Mathematical Theory of Induced Voltage in the High-Tension Magneto. Bureau of Standards Scientific Paper No. 424; 1921. (See p. 457 for details of this method.)

10. F. B. Silsbee: Scientific Paper No. 424, p. 452. Bureau of Standards; 1921.

11. F. B. Silsbee: Scientific Paper No. 424, p. 427, equation 27. Bureau of Standards; 1921.

12. F. B. Silsbee: Simplified Theory of the Magneto. N. A. C. A. Technical Report No. 123; 1921. Scientific Paper No. 424, pp. 426–437. Bureau of Standards; 1921.

13. F. B. Silsbee: Scientific Paper No. 424; Sections II and III. Bureau of Standards; 1921.

14. Taylor–Jones, E.: Phil. Mag., 36, p. 145; 1919.

15. H. Armagnat: Revue Electrique, 23, p. 321; 1915.

16. Taylor–Jones, E.: Phil. Mag. 36, p. 145; 1918.

17. F. B. Silsbee: Scientific Paper No. 424: Sections II and III. Bureau of Standards; 1921.

TABLE 1

MECHANICAL AND MISCELLANEOUS CHARACTERISTICS

1	2	3	4	5	6	7	8	9	10	11	12
System	Number of cylinders	Flux changes per revolution	Sparks per revolution	Angle on cam that breaker is closed	Angle on cam that breaker is open	Percentage of time that breaker is closed	Timing range (on engine crankshaft)	Angle from zero flux to break at full advance	Primary emf due to rotation at 1,000 R. P. M. effective value	Primary emf due to rotation at 1,000 R. P. M. crest value	Crest factor of emf of rotation
				Degrees	*Degrees*		*Degrees*	*Degrees*	*Volts*	*Volts*	
A—inductor	8	4	4	50	40	55	0	30	12.8	32	2.5
B—inductor	6 or 12	4	2 or 4	60	30 or 120	67 or 33	30	10	17.0	59	3.5
C—shuttle	4	2	2	154	26	85	34	12	12.4	49	4.0
D—revolving magnet	4	2	2	105	75	58	35	20	6.2	25	4.0
E—sleeve	8	4	4	30	60	33	0	21 or 10	8.8	30	3.4
F—inductor	4	4	2	58	122	32	30	7	18.0	46	2.5
G—pulsating flux	4	4	2	56	124	31	30	20	9.5	21	2.2
H—6-volt coil	8	[1]8	8	30	15	67					
I—6-volt coil	4	[1]4	4	45	45	50					
J—12-volt coil	4	[1]4	4	45	45	50					
K—shuttle	4	2	2	150	30	17	35	5	(2)	(2)	(2)

[1] Per revolution of cam. [2] Not measured.

TABLE 2

WINDING CHARACTERISTICS

1	2	3	4	5	6	7	8	9	10
System	Primary turns	Secondary turns	Effective ratio of turns n	Coupling coefficient $k^2=M^2/L_1L_2$	Leakage coefficient $1-k^2$	Resistance of primary winding at 20° C.	Resistance of secondary winding at 20° C.	Inductance of secondary winding at advance measured ballistically for high [4] speeds	Inductance of secondary winding at advance measured ballistically for low [5] speeds
						Ohms	*Ohms*	*Henrys*	*Henrys*
A—inductor	300	13,500	44.9	0.936	0.064	0.77	4,130	(1)	(1)
B—inductor	300	10,200	34.0	.936	.064	.72	1,850	55.6	50.0
C—shuttle	210	7,800	37.2	.961	.039	.67	2,350	53.2	52.5
D—revolving magnet	160	12,300	77.0	.932	.068	.30	8,540	132.0	122.0
E—sleeve	140	9,500	68.4	.972	.028	.51	1,960	84.6	82.0
F—inductor	[3]234	9,400	40.2	.966	.034	.48	2,660	69.8	68.0
G—pulsating flux	[3]211	13,500	64.1	.954	.046	.64	3,880	109.0	128.2
H—6-volt coil	240	13,600	56.6	.825	.175	.96	1,720	15.9	15.9
I—6-volt coil	145	11,300	78.2	.922	.078	1.04	4,270	39.8	39.8
J—12-volt coil	[3]325	10,900	33.6	.940	.060	2.50	3,900	36.2	36.2
K—shuttle	130	9,900	76.1	.996	.004	.50	2,730	72.2	76.1

1	11	12	13	14	15	16	17	18
System	Inductance of secondary winding at advance measured with low-frequency alternating current	Inductance of secondary winding at advance measured at 3,000 cycles	Resistance of secondary winding at advance measured at 3,000 cycles	Impulsive impedance referred to secondary $Z_t=\sqrt{L_t/C_o}$ computed for 50 R. P. M. assuming no losses	Impulsive impedance referred to secondary $nZ_m=n\,V_m/I_b$ mean of values observed at low speeds	Ratio of columns 15 to 14 $F=\dfrac{nZ_m}{Z_t}$	Frequency of main oscillation based on inductance given in column 10	Time-constant of primary circuit
	Henrys	*Henrys*	*Ohms*	*Ohms*	*Ohms*		*Cycles per second*	*Second*
A—inductor	30.0	17.0	115,000	500,000	250,000	0.50	1,500	
B—inductor	18.0	13.0	81,000	500,000	250,000	.50	1,410	
C—shuttle	22.0	9.3	148,000	470,000	170,000	.37	1,100	
D—revolving magnet	43.0	[2]26.0	[2]76,500	880,000	440,000	.50	1,590	
E—sleeve	37.0	[2]11.0	[2]304,000	840,000	350,000	.42	1,350	
F—inductor	33.5	15.0	170,000	580,000	180,000	.31	1,220	
G—pulsating flux	(1)	(1)	(1)	900,000	490,000	.54		
H—6-volt coil	15.6	14.5	45,500	330,000	250,000	.75	3,330	0.0040
I—6-volt coil	32.0	21.0	132,000	540,000	260,000	.48	2,130	.0053
J—12-volt coil	29.5	19.0	109,000	340,000	220,000	.64	1,510	.0071
K—shuttle	37.0	20.0	175,000	720,000	270,000	.37	1,550	

[1] Not measured.
[2] At 2,500 cycles per second.
[3] Data supplied by maker.
[4] For value of current equal to that observed at break at 2,000 sparks per minute.
[5] For value of current equal to that observed at break at 50 R. P. M.

TABLE 3

MAGNETIC CHARACTERISTICS

1	2	3	4	5	6	7	8	9	10	11	12
System	Maximum change in primary flux turns	Maximum flux through core	Weight of magnets	Cross-section of magnets	Length of magnet	Density of useful flux in magnet	Maximum possible current	Maximum possible energy per spark	Stored break 2,000 sparks per minute at advance	Stored break 50 R. P. M. at advance	Maximum observed heat per spark at advance
	Maxwell-turns	*Max-wells*	*Kilo-grams*	*Cm.²*	*Centi-meters*	*Gausses*	*Amperes*	*Joule*	*Joule*	*Joule*	*Joule*
A—inductor	11.6 x 10⁶	19,300	1.33	5.6	28.0	3,400	(¹)	(¹)	(¹)	(¹)	0.048
B—inductor	13.3	22,200	2.44	11.2	26.4	2,000	3.0	0.185	0.150	0.026	.130
C—shuttle	21.1	50,000	2.24	7.8	34.0	6,400	6.3	.650	.210	.061	.180
D—revolving magnet	9.0	28,000	1.14	7.5	16.0	3,700	5.0	.226	.114	.017	.076
E—sleeve	8.0	28,600	1.98	7.0	33.5	4,100	5.7	.228	.071	.020	.066
F—inductor	19.0	40,500	2.08	10.6	23.8	3,800	4.3	.420	.257	.086	.162
G—pulsating flux	9.6	45,500	1.35	8.9	18.3	5,100	5.9	.280	³.106	.010	.096
H—6-volt coil	1.9	7,900	--------	²1.77	²9.0	--------	3.8	.036	.036	.036	.029
I—6-volt coil	3.3	22,800	--------	²6.7	--------	--------	5.0	.082	.072	.082	.033
J—12-volt coil	7.6	23,400	--------	²6.7	--------	--------	2.4	.091	.069	.091	.037
K—shuttle	10.0	38,500	1.89	6.8	33.4	5,700	10.0	.520	.095	.017	(¹)

¹ Not determined. ² Dimensions of core. ³ At retard.

TABLE 4

CAPACITANCE DATA

1	2	3	4	5	6	7
System	Capacitance of primary condenser C_1	Capacitance of primary condenser referred to secondary C_1/n^2	Capacitance between core and inner layer of winding C_g	Internal capacitance among layers of windings C_w	Terminal capacitance between outer layer and frame C_t	Total effective capacitance referred to secondary C_e
	Microfarad	*Micro-micro farads*	*Micro-micro farads*	*Micro-micro farads*	*Micro-micro farads*	*Micro-micro farads*
A—inductor	0.060	30	250	100	³15	180
B—inductor	.098	85	290	75	³16	200
C—shuttle	.230	166	(⁵)	²50	¹25	260
D—revolving magnet	(⁵)	(⁵)	(⁵)	75	³31	⁴160
E—sleeve	.21	45	(⁵)	35	¹25	120
F—inductor	.19	118	280	50	³17	200
G—pulsating flux	.16	39	130	60	³42	160
H—6-volt coil	.26	81	110	40	³4	140
I—6-volt coil	.24	39	30	50	¹29	140
J—12-volt coil	.24	213	50	50	³29	310
K—shuttle	.13	22	230	60	³48	150

¹ Estimated from dimensions.
² From assumed C_t and observed ($C_w + C_t$) at radio frequency.
³ From audio frequency bridge.
⁴ Estimated.
⁵ Inaccessible

TABLE 5

DATA ON ENERGY VALUES AT LOW SPEEDS

1	2	3	4	5	6	7	8	9	10	11
System	Primary current at break at 50 R. P. M. at advance	Secondary crest voltage at 50 R. P. M. at advance	Stored magnetic energy at break at 50 R. P. M. at advance	Heat per spark at 50 R. P. M. at advance (estimated from data at high speed)	Crest value of electrostatic energy at 50 R. P. M. at advance	Energy efficiency as a coil $\frac{C_o V_m^2}{2W}$	Time-constant of eddy circuit at 3,000 cycles (T_e)	Coefficient of coupling between coils and eddy circuit at 3,000 cycles (k_e^2)	Theoretical voltage efficiency using constants observed at 3,000 cycles	Observed voltage efficiency at 50 R. P. M. at advance
	Amperes	Volts	Joule	Joule	Joule		Second			
A—inductor	0.52	7,000	(1)	0.013	0.0044	--------	0.000119	0.53	0.75	--------
B—inductor	1.10	8,000	0.026	.013	.0064	0.25	.000067	.48	.81	0.50
C—shuttle	1.80	8,600	.061	.011	.0074	.12	.000086	.85	.49	.35
D—revolving magnet	1.30	8,600	.017	.007	.0059	.35	[2].000240	[2].41	[2].80	.59
E—sleeve	1.50	8,000	.020	.006	.0037	.18	[2].000130	[2].91	[2].46	.42
F—inductor	2.05	9,000	.086	.012	.0081	.09	.000105	.67	.68	.30
	.80	6,500	.010	.008	.0033	.33	(1)	(1)	(1)	.57
	3.80	17,700	.036	.029	.0220	.61	.000023	.40	.89	.78
	4.96	15,900	.082	.033	.0250	.31	.000083	.47	.80	.56
	2.38	14,200	.091	.036	.0310	.34	.000098	.51	.78	.58
K—shuttle	1.60	6,500	.017	(1)	.0031	.18	.000100	.59	.72	.42

[1] Not measured.   [2] At 2,500 cycles per second.

TABLE 6

DATA ON OPERATION WITH SHUNTING CONDUCTANCE

1	2	3	4	5	6	7	8	9	10	11
System	Conductance (1/S) for 5,000 volts at 2,000 sparks per minute at advance	Shunting resistance (S) for 5,000 volts at 2,000 sparks per minute at advance	Crest value of current resistance at 2,000 sparks per minute computed from observed voltage	Current at break per minute at advance referred to secondary I_b/n	Quotient of columns 4 and 5	Crest value of current through shunting resistance at 2,000 sparks per minute computed by double-coil model from current at break	Energy lost in shunting resistance during rise of voltage [1]	Crest value of electrostatic energy at 5,000 volts	Total energy required per spark at 5,000 volts with conductance given in column 2	Stored magnetic energy at break at 2,000 sparks per minute at advance
	Micromhos	Ohms	Ampere	Ampere		Ampere	Joule	Joule	Joule	Joule
A—inductor	5	200,000	0.025	0.037	0.68	--------		0.0022	--------	(²)
B—inductor	19	53,000	.094	.073	1.29	0.112	.040	.0025	0.043	0.150
C—shuttle	33	30,000	.165	.089	1.85	.142	.073	.0032	.076	.209
D—revolving magnet	8	125,000	.040	.041	.98	.064	.023	.0020	.025	.114
E—sleeve	14	71,000	.070	.041	1.70	.066	.027	.0015	.029	.071
F—inductor	23	43,000	.116	.086	1.35	.136	.053	.0025	.026	.257
G—pulsating flux	[3]20	[3]50,000	[3].100	[3].056	[3]1.80	[3].098	[3].051	[3].0020	[3].053	[2,3].106
H—6-volt coil	18	55,000	.091	.067	1.36	.091	.017	.0018	.019	.036
I—6-volt coil	13	78,000	.064	.060	1.07	.090	.019	.0017	.021	.072
J—12-volt coil	16	67,000	.080	.062	1.29	.099	.033	.0038	.037	.069
K—shuttle	15	67,000	.075	.051	1.47	.068	.030	.0018	.032	.095

[1] Assuming frequency given in column 17, Table 2.   [2] Not measured.   [3] At retard.